CT and MRI in Ovarian Carcinoma

10

Rosemarie Forstner

CONTENTS

R. Forstner, MD
PD, Department of Radiology, Landeskliniken Salzburg, Paracelsus Private Medical University, Müllner Hauptstrasse 48, 5020 Salzburg, Austria

10.1 General Considerations

The vast majority of ovarian carcinomas are epithelial in origin, accounting for more than 90% of the estimated 25,580 new cases of ovarian cancer diagnosed in 2004 in the United States [1]. Fallopian tube carcinomas and extraovarian peritoneal carcinomas are much less common. However, these tumors share similarities in histology, tumor growth, treatment, chemotherapy responsiveness, and overall prognosis. For this reason, most aspects of these tumors will be discussed under epithelial ovarian cancer in this chapter. For both epithelial and fallopian tube cancer, there are significant differences in the prognosis between early and advanced ovarian cancer. While early-stage cancer is often curable, advanced-stage ovarian cancer is one of the most deadly cancers in women, with an overall 5-year survival rate of 38%–53% [1].

10.2 Epidemiology and Risk Factors

Ovarian cancer accounts for 4% of cancers in women and is responsible for 5% of cancer deaths [2]. In most Western countries, ovarian cancer is the sixth most common cancer in women, and the most lethal among the gynecological cancers. The incidence of ovarian cancer has increased by 30% over the past decade, while death from ovarian cancer has increased by 18% [3]. It is estimated that one women in 70 will develop ovarian cancer, and one woman in 100 will die of the disease. Ovarian cancer is usually clinically silent and about 75% of women present with advanced stages. This is why, despite developments in diagnosis and treatment, the overall survival rate has changed only little within the last decade [4]. Although there is an

initial response in most patients, the majority ultimately will die from their disease [3].

The incidence of ovarian cancer is higher in North America and Northern Europe than in Japan [3]. The strongest patient related risk factor for ovarian cancer is increasing age. The vast majority of epithelial ovarian carcinomas are diagnosed in the postmenopausal period, with a mean age at diagnosis of 59 years.

In patients with a family history of breast and ovarian cancer, ovarian cancers occur up to 10 years earlier. In females younger than 20 years of age, germ cell tumors account for more than two-thirds of malignant ovarian tumors.

Genetic, reproductive, and environmental factors have been identified to play a role in the development of ovarian cancer. The vast majority of ovarian cancers are sporadic in nature. Patients with a family history are at high risk, although an identifiable genetic predisposition for hereditary ovarian cancer is found only in approximately 5% of affected women. Families with three or more first-degree relatives with ovarian and/or ovarian and breast cancer carry a substantially (16%–60%) increased risk for developing ovarian cancer.

Hereditary breast-ovarian cancer syndrome (HBOC) accounts for the vast majority (85%–90%) of all hereditary ovarian cancers [5]. The site-specific ovarian cancer syndrome with only ovarian cancer accounts for 10%–15% of hereditary ovarian cancers. In hereditary nonpolyposis colorectal cancer syndrome (HNPCC), which is also known as Lynch syndrome II, patients present with colon, endometrial, breast, ovarian and other cancers [6].

The hereditary breast/ovarian cancer syndrome, and perhaps less frequently the site-specific ovarian cancer syndrome, are linked to mutations in the *BRCA1* and *BRCA2* genes [4]. The vast majority of *BRCA1*-associated cancers are serous adenocarcinomas and present at an average age at diagnosis of 48 years. *BRCA1*-associated cancers may have a longer median survival than sporadic ovarian cancer [4].

Women with nulliparity, childbirth after 35 years, late menopause, and early onset of menses are also under an increased risk. Prolonged times of uninterrupted ovulations seem to play a role in the development of ovarian cancer [3].

Treatment with ovulation stimulation drugs may also slightly increase the risk of developing ovarian cancer [3].

Long term oral contraceptive use, however, has been associated with a protective effect.

10.3 Screening for Ovarian Cancer

10.3.1 General Population

Successful screening for ovarian cancer, by definition, is able to decrease mortality and morbidity from the disease. Clinical palpation, transvaginal sonography, and serum CA-125 have been proposed as screening tests for ovarian cancer. Unfortunately, with these tests, routine screening for ovarian cancer is currently not recommended in the general population [3, 4, 7].

Successful screening for ovarian cancer requires either detection of early invasive stage disease or of a precancerous stage [4]. Although the patterns of spread of ovarian cancer are well established, its natural course is poorly understood. It seems that the preclinical phase of ovarian cancer may last less than 2 years [7]. Furthermore, most ovarian cancers, particularly serous types, may develop without a precursor lesion, which makes early detection difficult [8].

The primary reason that screening is not recommended, however, is based upon the fact that the currently available techniques have not shown to decrease the mortality of ovarian cancer in large clinical screening trials [3]. The detection rate of ovarian cancer is low, and cost-benefit analysis of ovarian cancer screening is currently not cost-effective [9]. Most screening studies have used either serum tumor markers or ultrasonography including color Doppler imaging, or both. Although US has excellent reported sensitivity and specificity for detection of ovarian masses (90%-96% and 98%-99%, respectively), its PPV is only about 7% for ovarian cancer, mainly because of its low prevalence. Serum CA-125 levels correlate with progression or regression of established disease. This test, however, is not specific and is found in benign diseases as well. False-positive findings during screening may even lead to adverse effects with an increased morbidity due to unnecessary surgeries [10].

10.3.2 High-Risk Women

Screening may be more effective in women with a positive family history of ovarian cancer. The American College of Radiology (ACR) recommends that women with a strong family history of ovarian cancer should consult gynecologists in their early twenties

and undergo a clinical follow-up in their thirties [7]. Because of the markedly increased lifetime risk of ovarian cancer, screening with annual transvaginal US and CA-125 testing is recommended for women with *BRCA1* or *BRCA2* gene mutations [11]. Prophylactic oophorectomy seems to have a protective effect in women from families with hereditary cancer. Oophorectomy may be delayed until childbearing is completed, or the age of 40. However, these patients carry a persisting risk for peritoneal carcinomatosis even after removal of normal ovaries [4].

10.4 Histologic Tumor Types and Tumor Grade

On the basis of distinct clinical and pathologic features, primary ovarian carcinomas can be separated into three major entities: epithelial carcinomas, germ cell tumors, and stromal carcinomas. Epithelial ovarian cancer accounts for 86% of tumors, the vast majority of ovarian malignancies [12]. Epithelial ovarian cancers are adenocarcinomas and comprise, depending on their histopathologic features, serous, mucinous, endometrioid, transitional cell, clear cell, undifferentiated carcinomas, and mixed carcinomas. Fallopian tube cancers show similar histologies, with serous carcinoma also identified most frequently [3]. Except for clear cell carcinomas, the histologic type has limited prognostic significance independent of clinical stage [3].

Epithelial carcinomas are characterized by histologic type and the degree of cellular differentiation (grade). Most grading systems are based upon a three-grade classification that describes the degree to which a tumor forms papillary structures or glands vs solid tumors [4]. At present, grading of ovarian carcinoma is clinically relevant only for stage I tumors, because of its direct impact on the necessity of chemotherapy and the prognosis [2].

10.5 Tumor Markers

CA-125, a glycoprotein antigen, is currently the most commonly used tumor marker for ovarian cancer. However, elevation of CA-125 of more than 35 U/ml is not specific for epithelial ovarian cancer, but can be observed as well in other malignant epithelial cancers, including pancreatic, lung, breast, and colon cancer, and in non-Hodgkin's lymphoma [13]. Furthermore, the list of benign conditions associated with an elevated CA-125 level is long and includes cirrhosis, peritonitis, pancreatitis, endometriosis, uterine fibroids, pregnancy, benign ovarian cysts, pelvic inflammatory disease, and even ascites. The level of CA-125 is associated with the menstrual cycle, and more than 90% of false-positive findings are encountered in premenopausal women [14]. This is why in premenopausal women, CA-125 is not useful as a single test, but its value is based upon the rise in serial measurements. In postmenopausal women, CA-125 is a better discriminator between benign and malignant diseases. In this age group, CA-125 levels exceeding 65 U/ml are predictive of malignancy in 75% of women with pelvic masses [7]. More than 80% of women with advanced epithelial ovarian cancer present with CA-125 elevations. It is, however, not a sensitive test for early-stage disease, where its sensitivity is only 25% [14]. In mucinous ovarian cancers, the CA-125 levels may not be markedly elevated [15].

CA-125 is pivotal in the follow-up of patients with ovarian cancer to monitor efficacy and duration of treatment and tumor recurrence [16].

Serum alpha-fetoprotein (AFP) and human chorionic gonadotropin (HCG) have been helpful in recognizing preoperatively the presence of an endodermal sinus tumor, embryonal carcinoma, choriocarcinoma, or a mixed germ cell tumor.

10.6 Imaging

10.6.1 Imaging Features of Ovarian Cancer

10.6.1.1 Characteristics of Malignant Ovarian Tumors

Most commonly used imaging features suggestive of malignancy are lesions size larger than 4 cm, thickness of wall or septa exceeding more than 3 mm, papillary projections, necrosis, partially cystic and solid internal architecture, a lobulated solid mass, and presence of tumor vessels (Fig. 10.1; Table 10.1) [17–21].

Contrast-enhanced studies in CT and MRI assist in tumor characterization, especially in the depiction of papillary projections and necrosis [17, 21]. None of

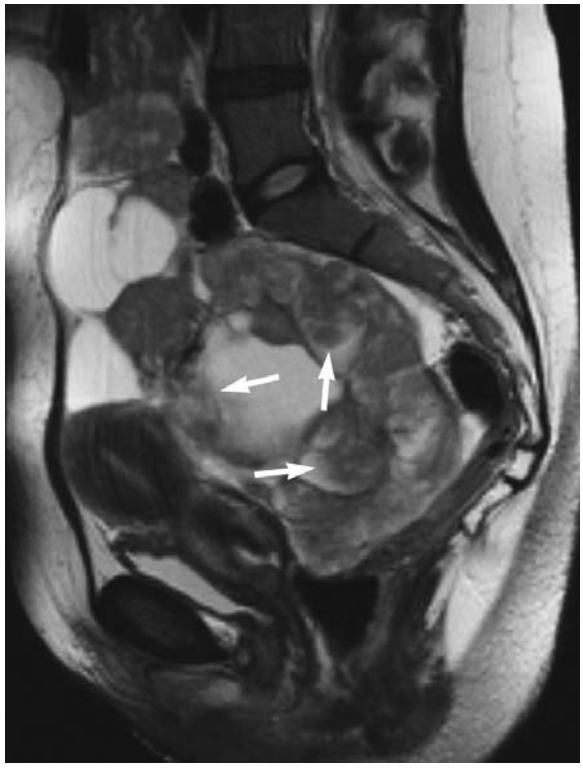

Fig. 10.1. Imaging characteristics of a malignant ovarian lesion. Sagittal T2-weighted image demonstrates a large adnexal lesion extending to above the umbilical level. It is clearly separated from the uterus and compresses the rectum. It is composed of multiple solid elements and multiple cysts. Throughout the lesion and within the cysts, papillary projections (*arrows*) can be identified. Histopathological diagnosis was a serous adenocarcinoma

Table 10.1. Imaging findings suggesting malignancy in an adnexal mass

Primary findings[a]
Lesion size >4 cm
Wall/septal thickness >3 mm
Papillary projections
Lobulated mass
Necrosis
Solid and cystic architecture
Tumor vessels
Ancillary findings
Lymph node enlargement
Peritoneal lesions
Ascites

[a]Not specific as single factors.

these imaging criteria, however, are specific enough as a single factor to reliably diagnose ovarian cancer. The likelihood of malignancy increases with solid nonfibrous elements, thickness of septa, and presence of necrosis. Ancillary findings such as presence of lymphadenopathy, peritoneal lesions, and ascites improve the diagnostic confidence to diagnose ovarian cancer. The combination of tumor size and architecture and ancillary signs improves prediction of malignancy and yields an accuracy of 89%–95% [19, 21].

Necrosis within a solid portion of an ovarian mass was most predictive sign of malignancy in a multivariate logistic regression analysis of complex adnexal masses studied by MRI (Fig. 10.2). "Necrosis in a solid lesion" (odds ratio, 107) was followed by "vegetations in a cystic lesion" (odds ratio, 40) identified after intravenous injection of gadolinium-based contrast material [21]. Solid nonfatty nonfibrous tissue with or without necrosis has also been reported as a valuable predictor of malignancy [22]. Thick walls and septations are less reliably signs of malignancy, as they may also occur in abscesses, endometriomas, and benign neoplasms such as cystadenofibromas and mucinous cystadenomas [22].

Papillary projections present folds of the proliferating neoplastic epithelium growing over a stromal core. Identification of papillary projections is impor-

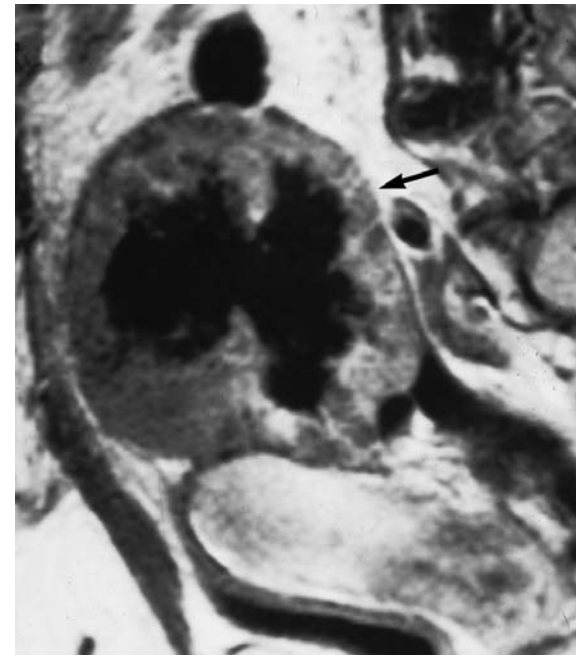

Fig. 10.2. Necrosis in Krukenberg tumor. Parasagittal contrast-enhanced T1-weighted image shows a well-delineated solid ovarian lesion (*arrow*) located cephalad of the uterus. It displays inhomogeneous contrast enhancement and a large central necrosis

tant because they are typical for an epithelial neoplasm. They are most often associated with epithelial cancers with low malignant potential, and may also be found in 38% of invasive carcinomas (Fig. 10.3). In the latter, the gross appearance is usually dominated by a solid component [17, 22].

Psammoma bodies, which are tiny calcifications, are found in CT in approximately 10% of serous epithelial ovarian cancers (Fig. 10.4). Calcifications are also found in benign ovarian stromal tumors, e.g., Brenner tumors or thecomas. These tumors are typically solid and tend to show extensive coarse calcifications.

10.6.1.2 Peritoneal Carcinomatosis

Peritoneal implants appear as solitary, or more often as multiple soft tissues lesions (Fig. 10.5), which display a wide range of size and patterns. Implants may be distributed along the peritoneal surfaces in a linear and often linear and nodular pattern (Fig. 10.6); they may also coalesce and surround the viscera or the diaphragm in a plaque- or coatlike manner. The majority of these implants enhance with contrast media; some are cystlike and may mimic loculated fluid. Implants from serous tumors may have calcifications (Fig. 10.7).

The omentum accounts for the most common sites of peritoneal metastases, with the inframesocolic omentum more often involved than the supramesocolic omentum. Most common types of omental implants include a netlike pattern, nodules of various sizes, and broad, bandlike soft-tissue lesions, an omental cake (Fig. 10.8). Nodular enhancing implants and omental cake are typically located between the abdominal wall and bowel loops.

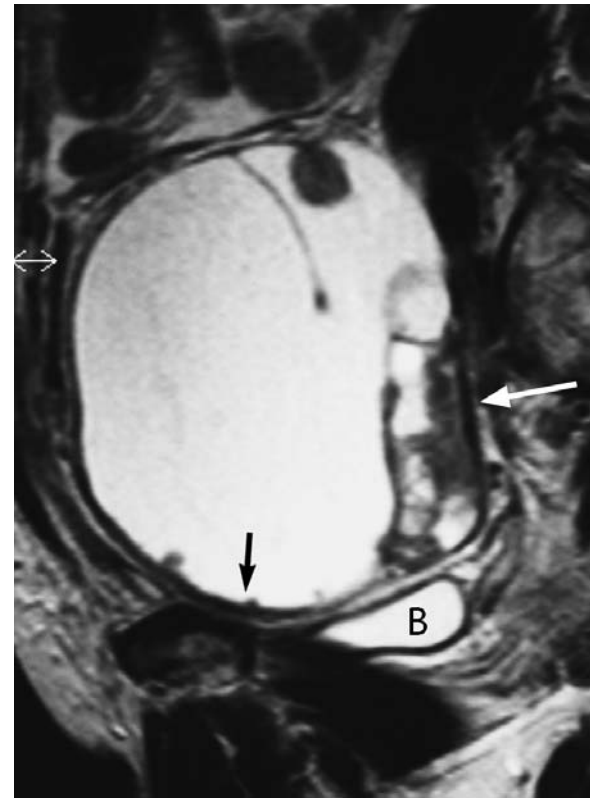

Fig. 10.3. Papillary projections in ovarian cancer. On a parasagittal T2-weighted image, a cystic ovarian lesion with septations and multiple papillary projections is demonstrated. Some small isolated papillary projections are located at the base of the lesion (*arrow*). At the top, a 1.5-cm papillary projection protrudes into the fluid-filled cavity. At the posterior aspect of the tumor, septal wall thickening and coalescence of papillary projections forming broad-based formations (*long arrow*) is demonstrated. Papillary projections typically display low signal intensity on T2-weighted image. *B*, bladder

Fig. 10.4. Calcifications in ovarian cancer. Multiple plaquelike calcifications are demonstrated within a mixed solid and cystic bilateral ovarian tumor. They also cloak the peritoneal surface of the uterus (*U*). These small calcifications present psammoma bodies and are found in approximately 10% of serous ovarian adenocarcinomas in CT. *B*, bladder

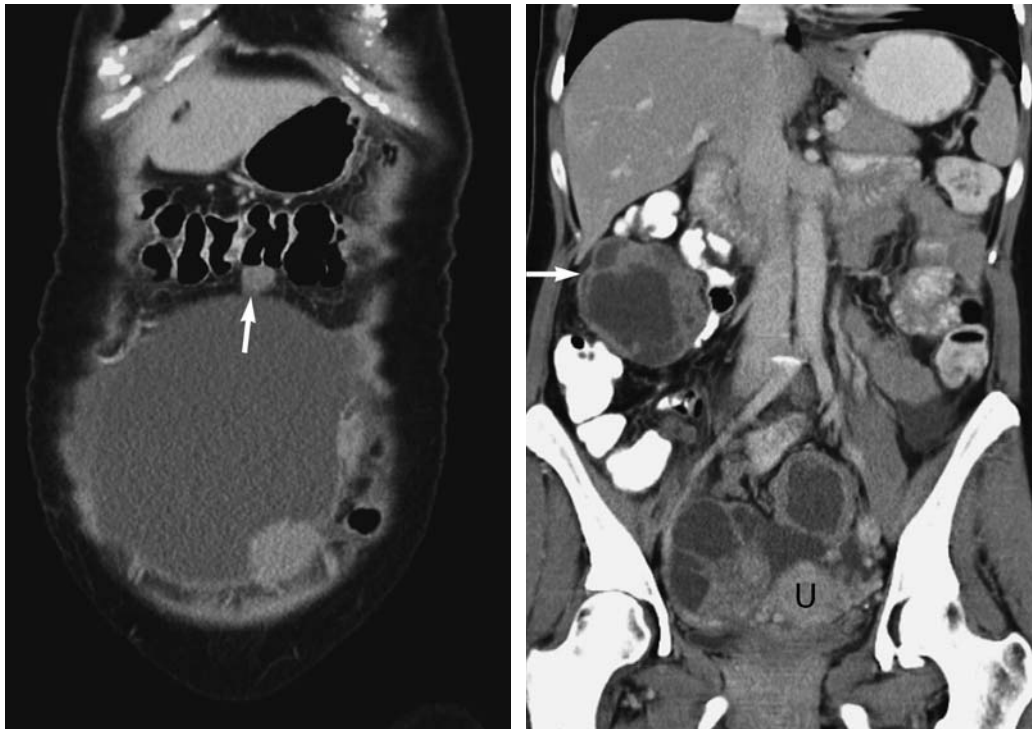

a b

Fig. 10.5a,b. Peritoneal implants. Findings in FIGO stage IIIc ovarian cancer are shown in an anterior (**a**) and posterior (**b**) coronal CT plane. Ascites, mild peritoneal thickening and multiple solid peritoneal implants along the anterior abdominal wall and in the transverse mesocolon (*arrow*) are demonstrated in **a**. A large implant in the right paracolic gutter (*arrow*) resembles the morphology of the thick-walled cystic and solid adnexal tumors, which present bilateral ovarian cancer (**b**). (*U*), uterus

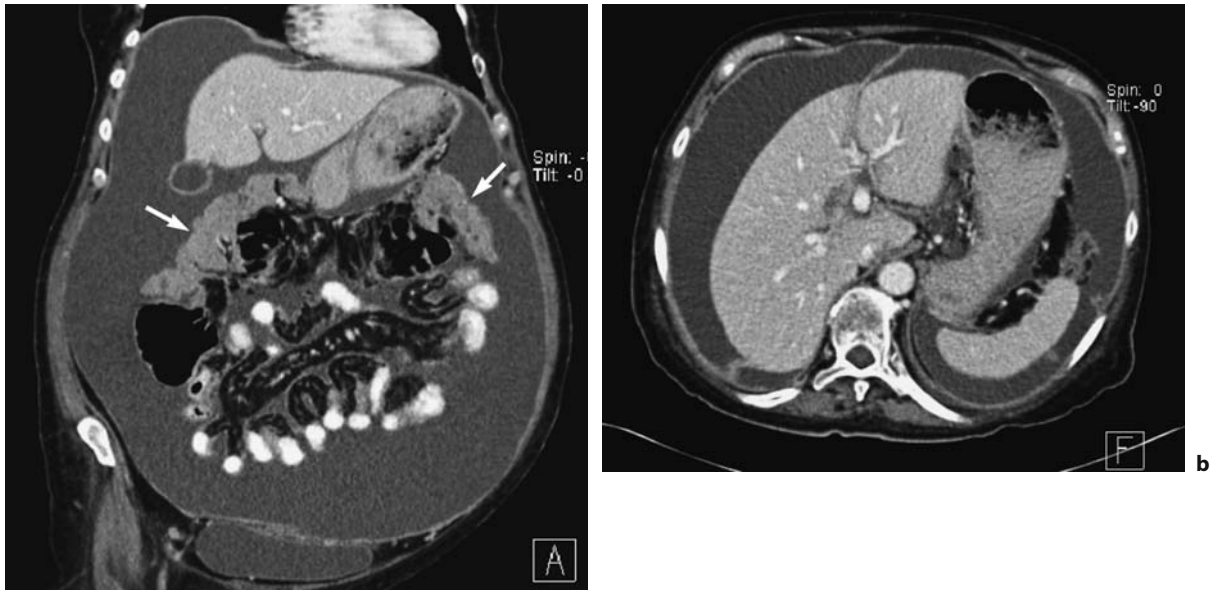

a b

Fig. 10.6a,b. Peritoneal implants. Coronal (**a**) and transaxial CT of the upper abdomen (**b**). Linear thickening of the parietal peritoneum is seen throughout the abdomen and pelvis in a patient with large amounts of ascites (**a**). The diffuse linear thickening of the diaphragm is better appreciated on the transaxial plane (**b**). Other findings include bilateral focal diaphragmatic implants and broad bandlike tumors (*arrows*) adjacent to the transverse colon presenting omental cake

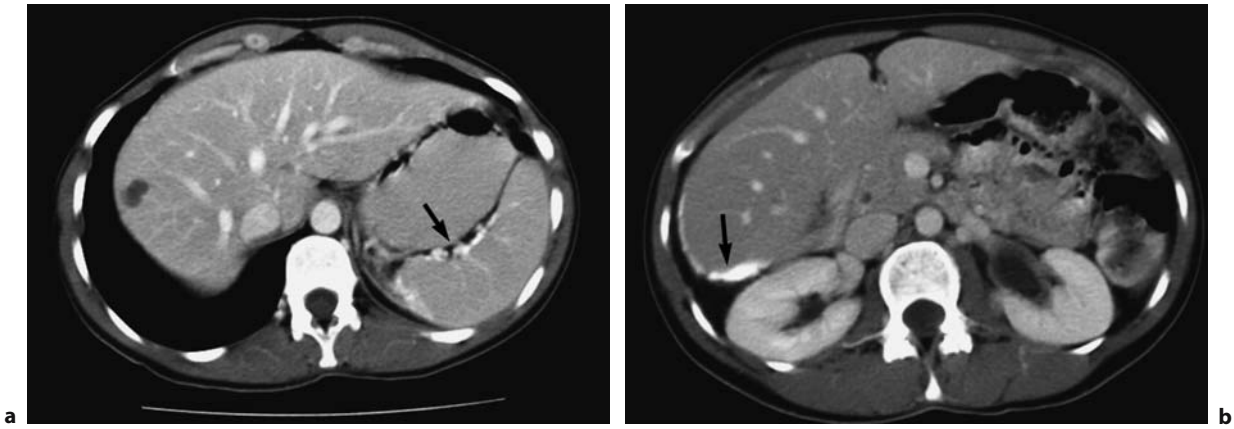

Fig. 10.7a,b. Calcified peritoneal metastases in CT. Multiple tiny calcifications (*arrows*) coat the surface of the spleen (**a**) and liver (**b**) in a patient with recurrent serous ovarian cancer. A simple cyst is found in the right lobe of the liver (**a**)

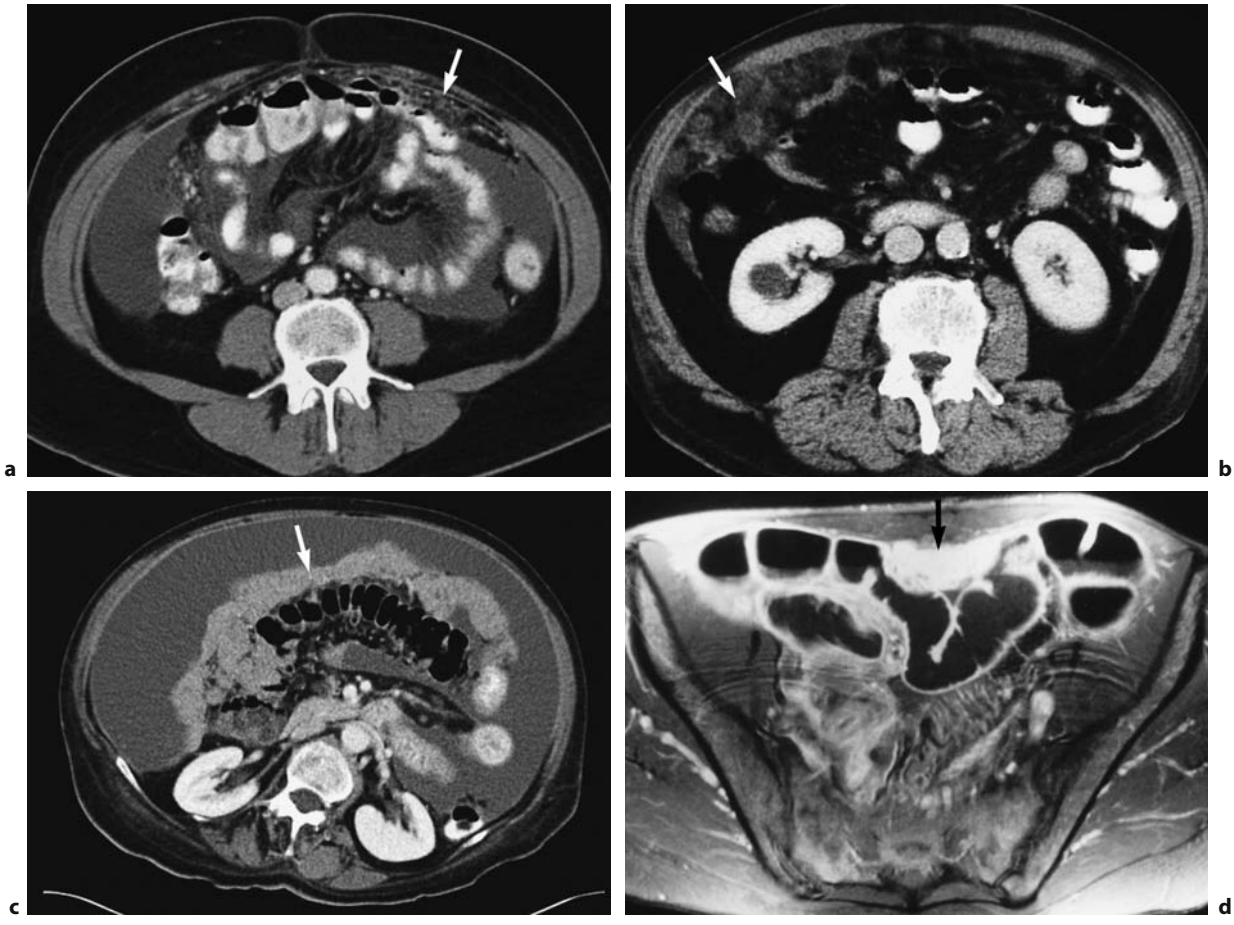

Fig. 10.8a–d. Omental implants. Transaxial CT (**a–c**) and transaxial fat-saturated T1-weighted image (**d**) in four different patients. Omental implants (*arrows*) may display a broad spectrum of findings ranging from a netlike pattern (**a**) to cottonlike (**b**) and nodular lesions (**d**). They are typically located between the abdominal wall and bowel loops. If they coalesce they are termed omental cake (**c**)

Netlike omental involvement is more difficult to evaluate. Implants of the diaphragm consist of nodular or plaquelike lesions. Peritoneal implants of liver or spleen may result in scalloping of the surface. Ligaments may appear thickened due to peritoneal metastases. Implants on bowel or mesentery can cause tethering of loops and may lead to obstruction. Bowel obstruction, however, results more commonly from intestinal wall involvement than from serous implants. Mesenteric lesions appear as thickening of the root of the mesentery, and often display a stellate radiating pattern.

Sister Mary Joseph's nodule presents metastatic cancer to the umbilicus. It usually ranges from 1 to 1.5 cm in size, but can attain a size of up to 10 cm (Fig. 10.9).

The depiction of peritoneal implants depends on the size and presence of ascites. The latter improves the conspicuity, especially of smaller lesions. However, implants less than 1 cm are detected with a sensitivity of only 25%-50% with spiral CT technique [23]. In this study, CT performance improved to a sensitivity of 85%-93% and a specificity of 91%-96% in detecting extrapelvic peritoneal disease larger than 1 cm in size [23]. Contrast-enhanced CT and MRI aid in the depiction of peritoneal implants. MRI seems similar to CT in the assessment of abdominal peritoneal implants and seems superior in the assessment of pelvic peritoneal details [24].

10.6.1.3 Ascites

Ascites alone is generally nonspecific, and small amounts of pelvic fluid are commonly detected in the cul-de-sac in normal patients. In ovarian cancer, pelvic ascites may be a sign of stage I disease; however, involvement of the diaphragmatic lymphatics, which presents stage III, should generally be a concern [25]. Large amounts of ascites in a patient with ovarian cancer usually indicate presence of peritoneal metastases. Coakley found that the presence of ascites alone had a PPV of 72%–80% for peritoneal metastases [23]. Furthermore, a direct relationship between stage of ovarian cancer and volume of ascites has been found [26]. Absence of ascites may not exclude a malignant disease, as 50% of borderline tumors and 83% of early-stage ovarian cancers are not associated with ascites [4]. Peritoneal carcinosis is characterized by various amounts of ascites and diffuse or focal peritoneal thickening. Benign forms of ascites displaying the same pattern such as postoperative inflammatory changes, bacterial peritonitis, or chronic hemodialysis cannot be differentiated from peritoneal carcinosis [27]. Absence of ascites in the cul-de sac in cases of ascites throughout the pelvis or abdomen has been described as a sign of malignancy [28].

10.6.2 Pathways of Spread in Ovarian Cancer

Knowledge of the pathways of tumor spread is pivotal for the interpretations of findings in CT and MRI, and they are the basis for staging of ovarian cancer.

Ovarian cancer spreads primarily by direct extension to neighboring organs by exfoliating cells into the peri-

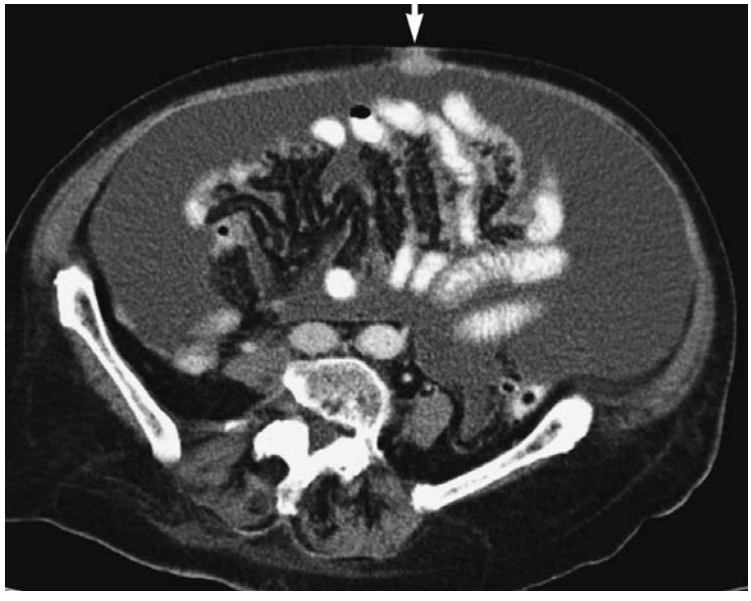

Fig. 10.9. Umbilical metastasis. Sister Mary Josef's nodule is a peritoneal implant to the umbilicus. In this patient, a solid 1.5-cm lesion (*arrow*) is demonstrated. Other signs of peritoneal tumor spread include large amounts of ascites and focal thickening of the peritoneum in the right paracolic gutter

toneal cavity that can implant on parietal and visceral peritoneum throughout the peritoneal cavity. It also disseminates by lymphatic pathways, and less commonly metastasizes hematogenously. Locoregional spread of ovarian cancer occurs by continuous growth along the surfaces of the pelvic organs and pelvic side walls. Peritoneal spread and implantation outside the pelvis is caused by tumor cells that are able to slough off the ovary and enter the peritoneal circulation. Peritoneal implants are also disseminated throughout the lymphatic vessels of the peritoneum. Due to the hemodynamics of the peritoneal fluid, the sites most often involved are the right subphrenic space, including the diaphragm, the liver surface, and Morrison's pouch. Further sites of peritoneal implants include the omentum, the surface of the left diaphragm and spleen, paracolic gutters, mesentery, and small and large bowel surfaces.

Tumor spread along the lymphatic pathways is found along three routes. The main pathway of lymphatic spread is along the broad ligament and parametria to the pelvic sidewall lymph nodes (external iliac and obturator chains), and along the ovarian vessels to the upper common iliac and para-aortic lymph nodes between the renal hilum and aortic bifurcation. Drainage to external and inguinal nodes via the round ligaments accounts for the rarest route of lymphatic tumor spread. At surgery, lymph node metastases are directly correlated with tumor stage: in stages I and II, 14% of lymph node metastases may be positive for metastases, whereas in stages III and IV, up to 64% of lymph node metastases are detected [29]. Furthermore, pelvic lymph nodes are more often involved than para-aortic nodes.

Hematogenous spread occurs later in the course of the disease. Distant metastases are most commonly found in the liver, lung, pleura, and kidneys. At the time of the initial presentation, parenchymal liver metastases are extremely rare, and patients are more likely to present with liver surface metastases [28].

10.6.3 Staging of Ovarian Cancer

Staging of ovarian cancer is based on the extent and location of disease noted at initial exploratory staging laparotomy. The most commonly used staging system of ovarian cancer is the International Federation of Gynecologists and Obstetricians (FIGO) classification system. Complete surgical staging has been established as the gold standard for assessing ovarian cancer. This procedure includes a staging laparotomy with a total abdominal hysterectomy, bilateral salpingo-oophorectomy, infracolic omentectomy, and lymphadenectomy [4, 29]. Furthermore, peritoneal cytology and multiple peritoneal biopsies are obtained throughout the pelvis and upper abdomen. More recently, laparoscopic staging procedures for ovarian cancer have also been proposed.

Understaging of ovarian cancer remains a common problem (20%–40%) in clinical routine. It occurs frequently, when the initial surgery had been performed under the presumption of a benign process, due to laparoscopy technique, and lack of oncologic specialist expertise [4].

10.6.3.1 Staging by CT and MRI

Surgical staging is regarded as the gold standard to evaluate a patient with ovarian cancer, and it is the basis to determine whether additional therapy is necessary [4]. Surgical staging can be preceded by a series of preoperative tests. Routine chest X-ray has been recommended to screen for lung metastases. Intravenous urography and contrast enema have previously been used in the preoperative evaluation of the urinary tract, and to exclude colon wall invasion or stenosis. Recently, CT and MRI have been widely accepted as adjunct imaging modalities for preoperative decision making in ovarian cancer [4, 11, 24, 30, 31].

Although definitive staging of ovarian cancer is based upon the findings at surgery, preoperative assessment of the tumor extent by imaging may influence patient management. Accurate preoperative assessment of ovarian cancer may aid the surgeon in better determining sites for biopsy, and also allow the depiction of tumor deposits that might be difficult to visualize intraoperatively, e.g., the diaphragm, splenic hilum, stomach, lesser sac, mesenteric root, and para-aortic nodes above the level of the renal hilum [4]. Furthermore, it may alert the surgeon of the need for subspecialist cooperation or for referral to an oncology center. In case of extensive cancer and signs of nonresectability on CT or MRI, candidates may be selected who may benefit from neoadjuvant therapy prior to surgery [15].

10.6.3.1.1 Imaging Findings According to Stages

A CT and MRI modified staging system of ovarian cancer is summarized in Table 10.2 [24, 25].

Table 10.2. Modified FIGO staging of ovarian cancer by CT and MRI

Stage	Imaging findingsa
Stage I	Tumor limited to the ovaries
IA	Limited to one ovary, no ascites (intact capsule and no tumor on the external surface)
IB	Limited to both ovaries, no ascites (as in stage IA)
IC	Stage IA or IB with ascites (or with tumor on surface). Capsule ruptured, peritoneal washings positive for malignant cells
Stage II	Growth involving one or both ovaries, pelvic extension
IIA	Extension and/or metastases to the uterus and/or fallopian tubes
IIB	Extension to other pelvic tissues
IIC	Tumor either IIA or IIB with ascites
Stage III	Tumor involving one or both ovaries, peritoneal implants (including liver surface, small bowel, and omentum) outside the pelvis and/or implants of retroperitoneal or inguinal lymph nodes
IIIA	Tumor grossly limited to the true pelvis (including microscopical implants of abdominal peritoneum)
IIIB	≤2 cm implants of abdominal peritoneal surfaces
IIIC	>2 cm implants of abdominal peritoneal surface and/or retroperitoneal or inguinal lymph nodes
Stage IV	Growth involving one or both ovaries, distant metastases, parenchymal liver metastases.

[a]Additional staging criteria used in histopathological and surgical staging in parentheses.

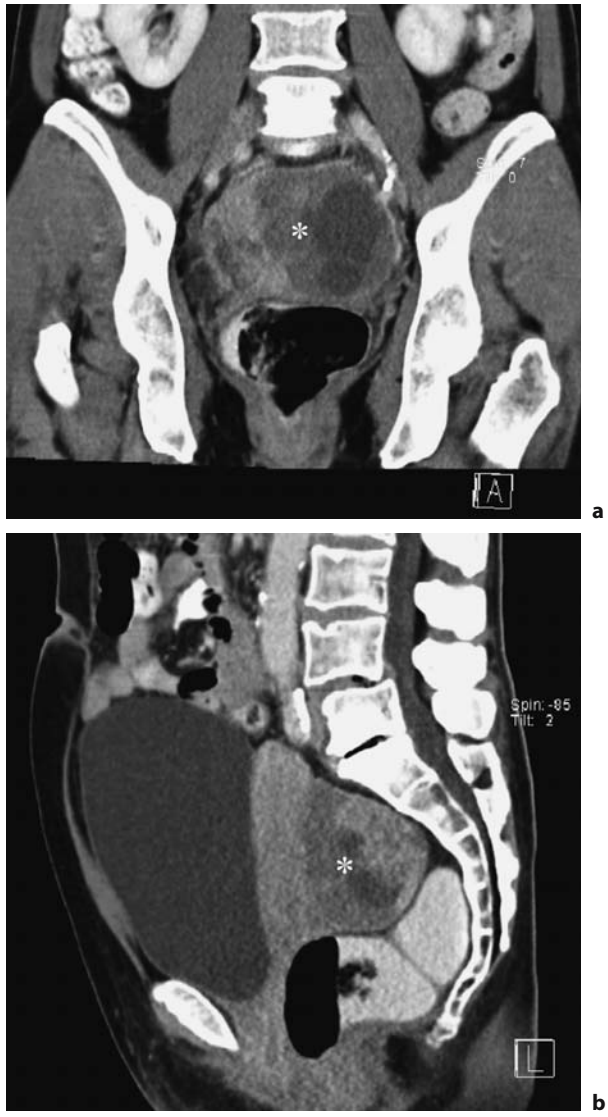

a

b

Fig. 10.10a,b. Stage I borderline tumor. Coronal (**a**) and parasagittal (**b**) CT. A 7-cm predominantly solid tumor (*asterisk*) with cystic areas is located in the cul-de-sac. The sagittal plane shows broad-based contact to the uterus (**b**). No evidence of ascites was found in the pelvis or abdomen. At surgery, a grayish tumor deriving from the left ovary was found. Histopathology revealed the rare endometrioid subtype of ovarian tumor of low malignant potential, which was classified as FIGO stage Ia

In stage I, tumor is confined to one (stage IA) or both ovaries (stage IB) (Fig. 10.10). The capsule of the tumor is intact and there is no evidence of spread of the tumor to the ovarian surface. In stage IC disease, tumor is detected on the ovarian surface or capsule rupture has occurred. Ascites may also be present.

Stage II is characterized by local tumor extension into the pelvic soft tissues and to organs within the true pelvis. In stage IIA, either direct tumor extension or implants on the uterus or fallopian tubes can be identified. Findings suggesting this stage include distortion or irregularity between the interface of the tumor and the myometrium. Stage IIB is characterized by involvement of pelvic tissues, such as bladder, rectum and pelvic peritoneum. Invasion of sigmoid colon or rectum is diagnosed when loss of tissue plane between the solid component of the tumor, encasement, or localized wall thickening is noted (Fig. 10.11). A distance of less than 3 mm between the lesion and the pelvic sidewall or displacement or encasement of iliac vessels is suggestive of pelvic sidewall invasion (Fig. 10.12). Stage IIC describes ovarian cancer as in stage IIA or IIB plus ascites.

Stage III consists of extrapelvic peritoneal implants and/or inguinal or retroperitoneal lymphadenopathy. Peritoneal lesions outside the pelvis, omental, or mesenteric implants are typical findings in stage III ovar-

ian cancer. Peritoneal tumor spread is characterized by peritoneal thickening or lesions projecting from the peritoneal surfaces, or lesions that are located within the mesentery or the omentum. Stages IIIA–IIIC differ in the size of abdominal peritoneal lesions. In Stage IIIA, tumor is grossly limited to the pelvis; however, large amounts of ascites are a sign of upper abdominal tumor spread. In stage IIIB, lesion size is 2 cm or less (Fig. 10.13); in stage IIIC it exceeds 2 cm (Fig. 10.5). Retroperitoneal and inguinal lymphadenopathy also constitute stage IIIC ovarian cancer. Ascites is a common finding in stage III disease; delayed enhancement of ascites was described as a sign of malignant ascites [32].

Stage IV ovarian cancer is characterized by distant metastases that include any location outside the pelvis, which is not spread peritoneally. Malignant pleural effusion is the most common clinical manifestation of stage IV ovarian cancer. Typical imaging findings include pleural effusion associated with pleural nodularity and focal pleural thickening (Fig. 10.14). Hematogenously spread metastases,

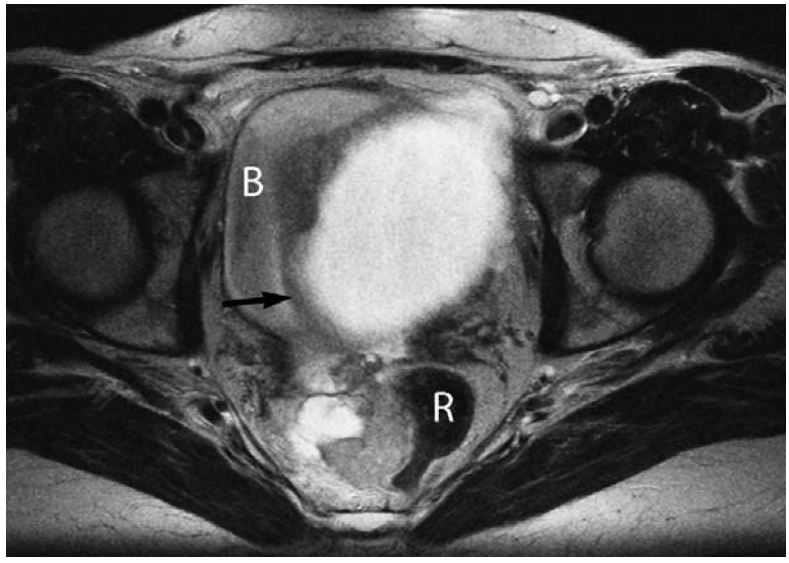

Fig. 10.11. Rectal wall invasion. Transaxial T2-weighted image. A cystic and solid left ovarian cancer (*arrow*) compresses bladder (*B*) and rectum (*R*). The latter shows broad contact with the solid tumor component located in the cul-de-sac. *B*, bladder

Fig. 10.12. Pelvic sidewall invasion. Transaxial CT at the level of the iliac bifurcation. A mixed solid and cystic adnexal tumor, which was nondifferentiated ovarian cancer at histopathology, is located in the pelvis. The left pelvic sidewall, including iliac vessels and psoas muscle, are clearly separated by fat. The right pelvic sidewall (*arrow*) is in direct contact with the solid tumor component. Furthermore, external and internal iliac arteries are displaced, the latter is encased by tumor (*arrowhead*)

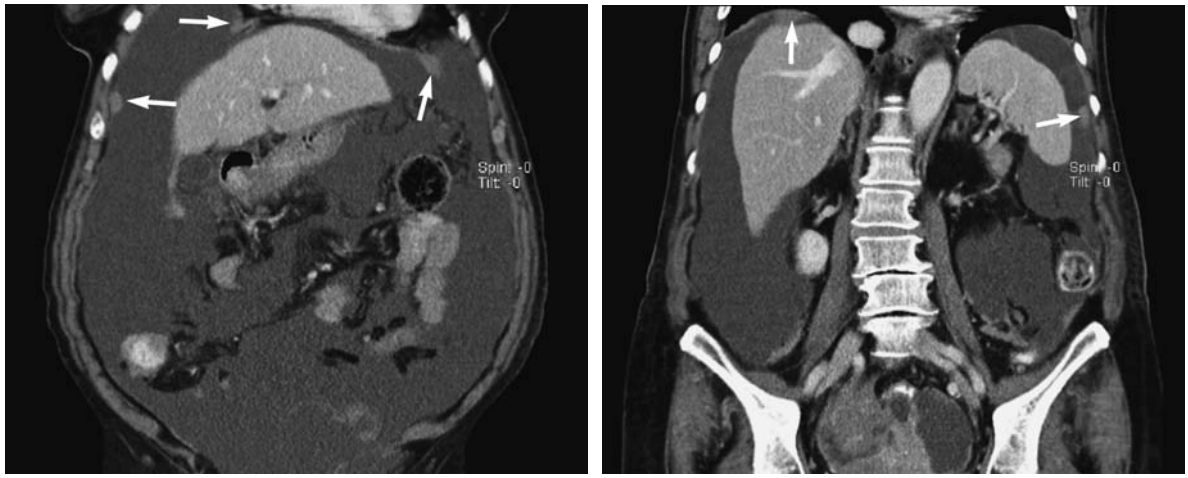

Fig. 10.13a,b. Stage IIIb ovarian cancer. Coronal CT at an anterior (**a**) and posterior level (**b**) demonstrate a pelvic ovarian mass and multiple small implants of the right and left diaphragm (*arrows*). Other findings include plaquelike and linear thickening of the peritoneum along the diaphragm, paracolic gutters, and in the pelvis (**b**). Because of large amounts of ascites, the peritoneal lesions can be well differentiated from adjacent anatomical structures

e.g., in the lung or liver parenchyma, are also typical manifestations in stage IV disease. It is particularly important to differentiate between liver surface metastases, which display smooth margins and an elliptic or biconvex shape, from liver parenchymal metastases (Fig. 10.15).

10.6.3.1.2 Value of Imaging

CT and MRI perform similarly in staging of ovarian cancer, with reported accuracy of 70%–90%, sensitivity of 63%–69% and specificity of 100% [23, 24, 25, 30, 33]. The decision to use CT or MRI is based on many factors, including cost, availability, contraindications, radiologist expertise, and clinician preference. CT is currently the primary imaging modality for staging ovarian cancer because of better availability and shorter examination times [24, 30]. Sensitivity for metastases declines with implant size less than 1 cm in diameter to 25%–50%. MRI may show advantages for detecting metastases within the pelvis. Helical CT improves the performance, with a reported sensitivity of 85%–93% and a specificity of 91%–96% for detection of peritoneal implants [23, 30]. Double-dose contrast-enhanced MR imaging including delayed images (5 min) may aid in the detection of subtle implants. In one study, this technique approximated the performance of laparotomy [16].

The diagnosis of lymphadenopathy is based on the short diameter of detectable lymph nodes. Based on a threshold of 1 cm or less in diameter the sensitivity for lymph node metastases is only 50%, and the specificity is 95% [34].

10.6.3.2 Prediction of Resectability

Cytoreductive surgery followed by chemotherapy is the cornerstone for the treatment of advanced ovarian cancer. Tumor debulking is generally considered successful or optimal when no residual tumor larger than 1–2 cm is left after the initial staging laparotomy [4]. A significant benefit in terms of response to chemotherapy and survival has been reported only in patients with residual tumor diameters of less than 2 cm [35]. Because of local anatomical limitations despite aggressive surgery, optimal cytoreduction rates range from 50% to 60%. Neoadjuvant chemotherapy followed by surgical debulking has been suggested as an alternative treatment approach in patients with bulky nonoptimally resectable disease [36]. This treatment option, however, is a complex issue and depends on the underlying medical condition of the patient, surgical risks, and expertise of the institution. Several studies have addressed the role of imaging in predicting resectability of patients with advanced ovarian cancer [24, 31, 27]. Identifying inoperable disease may help the surgeon to select candidates in whom chemotherapy seems the appropriate therapy. Resectability, as defined by imaging, is a function of location and size of peritoneal implants. Most commonly used

criteria indicating suboptimal cytoreduction include (a) retroperitoneal presacral implants, (b) lesions in the root of the mesentery, extensive disease (larger than 2 cm) along the undersurface of the diaphragm or lesser sac, liver surface implants in the gall bladder fossa, and interhepatic fissure, (c) suprarenal paraaortic lymph nodes, and d) liver parenchymal, pleural, and pulmonary metastases (Fig. 10.16) [24, 31]. Meyer et al. reported that inclusion of other factors such as ascites or CA-125 does not improve prediction and also suggested a scoring system [31]. CT and MRI performed with equal accuracy in detecting inoperable tumor and prediction of suboptimal debulking in ovarian cancer, with reported sensitivity of 76%, specificity of 99%, PPV of 99%, and NPV of 96% [37].

10.6.3.2.1 Value of Imaging

In the vast majority of patients, surgery remains the mainstay for treatment of ovarian cancer. It has been established that the maximal dimension of residual tumor remaining is an important prognostic factor. However, aggressiveness of surgery varies among the institutions and specialties. CT and MRI seem equally suitable to aid in patient management, especially to alert the surgeon to disease that may complicate the surgery or to the need of subspeciality assistance. Furthermore, imaging may aid in selecting patients with bulky unresectable disease who may benefit from neoadjuvant chemotherapy [37].

Fig. 10.14a,b. Stage IV ovarian cancer. CT in the pelvis (**a**) and lower thorax (**b**). At the time of diagnosis, the patient presented with bilateral ovarian tumors encasing the uterus (**a**). Furthermore, left cardiophrenic lymph node enlargement and a pleural mass (*arrow*) were found (**b**). Biopsy of the latter confirmed metastases from ovarian adenocarcinoma. No evidence of ascites or peritoneal dissemination was found at imaging and surgery

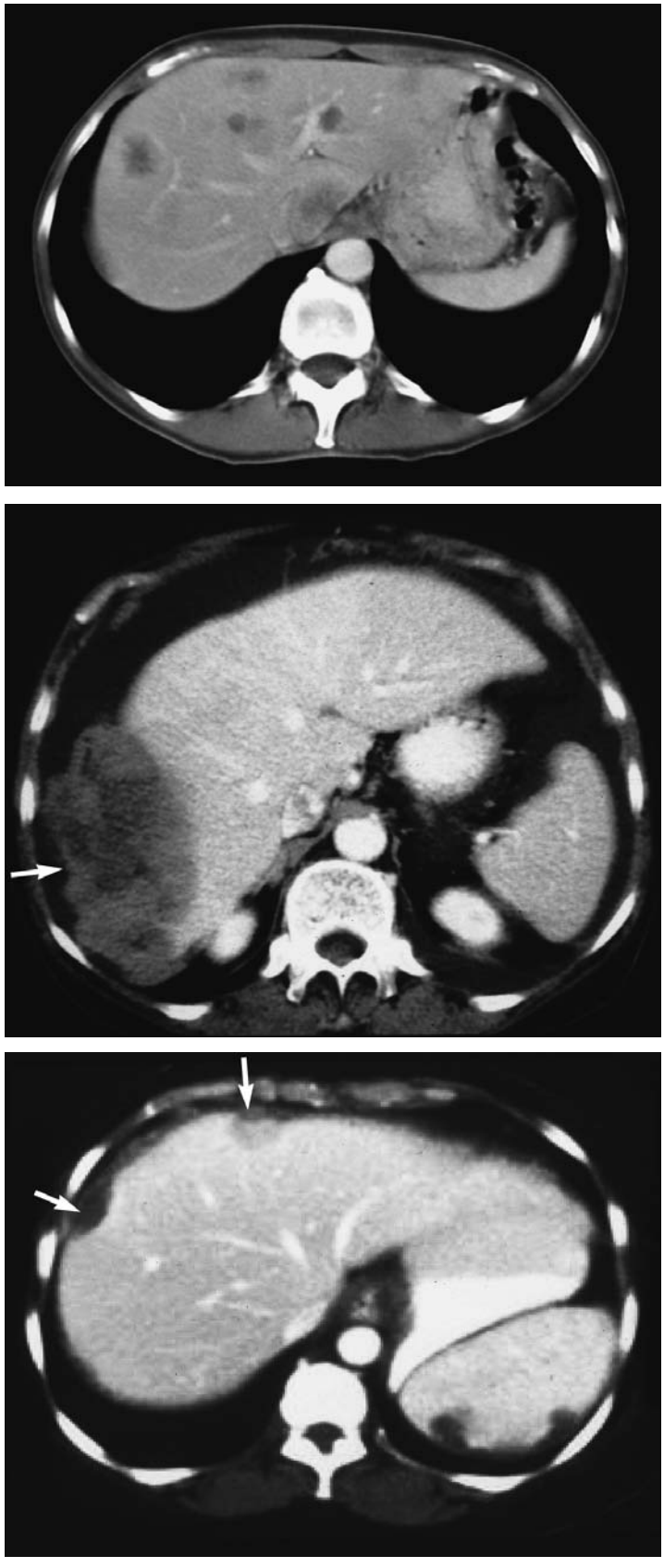

Fig. 10.15a–c. Spectrum of liver metastases in ovarian cancer. Transaxial CT shows multiple liver parenchymal metastases (**a**) and liver surface metastases (*arrows*) (**b**, **c**) in different patients with ovarian cancer. Liver surface metastases are typically crescent-shaped and may cause scalloping of the surface of the liver. Surface implants may be solid (**b**) or cystic (**c**). Splenic surface metastases are also found in **c**, which shows a morphology similar to the liver implants

10.6.4 Tumor Types

Patients with malignant tumors of the ovary and borderline tumors account for 21% and 4% of primary ovarian tumors, respectively [12]. Among these, epithelial cancer constitutes for the vast majority with 85%. Serous epithelial and mucinous ovarian cancer account for the majority of epithelial ovarian cancers and present approximately 49% and 36% of all ovarian epithelial tumors, respectively [3]. Endometrioid cell cancers account for 8%. The other cancers occur with equal frequency of 2% [3].

Malignant germ cell and malignant stromal neoplasm are responsible for 7% each. Germ cell tumors represent two-thirds of malignancies in females less than 20 years of age.

Unfortunately, there is a poor correlation between the gross appearance on pathology and the histologic type, and the aggressiveness cannot be determined on the basis of imaging studies.

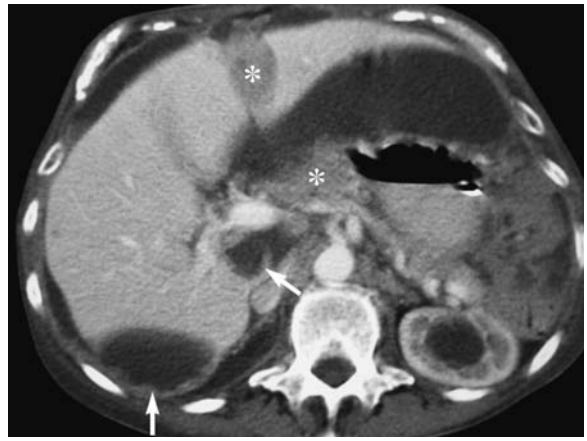

Fig. 10.16. Nonoptimally resectable ovarian cancer. Multiple peritoneal implants (*arrows*) are demonstrated on the liver surface and lesser sac. The latter is distended due to ascites. The implants located in the interlobar fissure (*asterisk*) and lesser sac (*asterisk*) are considered nonoptimally resectable

10.6.4.1 Epithelial Ovarian Cancer

10.6.4.1.1 Serous Ovarian Carcinoma

Serous adenocarcinoma is the most common type of ovarian cancer and accounts for approximately half of the epithelial ovarian cancers [2]. Two-thirds of these tumors involve both ovaries [2].

At macroscopy, serous adenocarcinomas appear typically as multilocular cystic tumors with intracystic papillary projections. These excrescences fill the cyst cavity, or they may contain serous, hemorrhagic, or turbid fluid (Fig. 10.17) [2]. Psammoma bodies within the tumor or implants, presenting tiny calcifications, are detected in 30% at histology, but only in 12% of cases in CT [38]. In up to 12% of women with advanced serous cystadenocarcinomas, the ovaries may be small and display predominantly surface involvement, warranting the diagnosis of primary carcinoma of the peritoneum [2].

10.6.4.1.2 Mucinous Adenocarcinomas

Mucinous cystadenocarcinomas comprise 36% of ovarian carcinomas. They tend to be large at diagnosis, and contain loculi with hemorrhagic or proteinaceous contents. Macroscopically, they present multiloculated cystic lesions with solid areas and intracystic nodules. Rarely, the tumor may be predominantly solid. Approximately 63% of mucinous adenocarcinomas are diagnosed as FIGO stage I tumors. Bilateral involvement is only found in 5%–10% [2]. Pseudomyxoma peritonei may be associated with mucinous adenocarcinomas. It consists of implants of mucinous contents on the abdominal and pelvic peritoneal surfaces.

10.6.4.1.3 Endometrioid Carcinomas

Endometrioid carcinomas represent 8% of all ovarian carcinomas. They occur with synchronous endometrial carcinomas or endometrial hyperplasia in up to 33% of cases [39]. Furthermore, an association with breast cancer has been reported [2]. Rarely, endometrioid carcinoma may arise from endometriosis [40]. Bilateral ovarian involvement is encountered in 30%–50% of cases. Macroscopically, these tumors are solid and cystic, the cysts may contain mucinous or greenish fluid. Rarely, solid tumors with extensive hemorrhage or necrosis may be found [2].

10.6.4.1.4 Clear Cell Carcinomas

Clear cell carcinomas present approximately 2%–7% of all ovarian cancers. Seventy-five percent of patients are diagnosed with stage I disease; however,

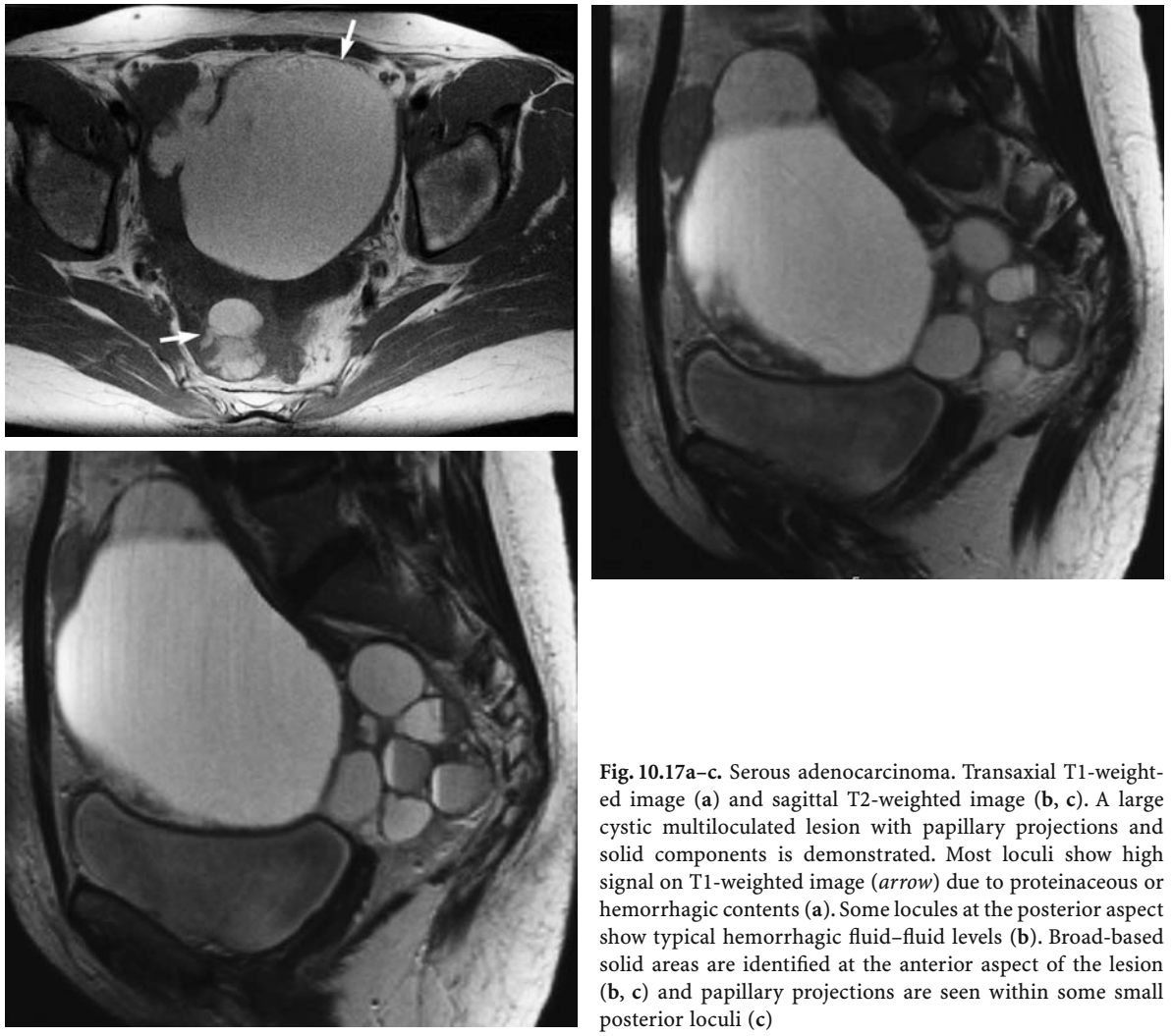

Fig. 10.17a–c. Serous adenocarcinoma. Transaxial T1-weighted image (**a**) and sagittal T2-weighted image (**b**, **c**). A large cystic multiloculated lesion with papillary projections and solid components is demonstrated. Most loculi show high signal on T1-weighted image (*arrow*) due to proteinaceous or hemorrhagic contents (**a**). Some locules at the posterior aspect show typical hemorrhagic fluid–fluid levels (**b**). Broad-based solid areas are identified at the anterior aspect of the lesion (**b**, **c**) and papillary projections are seen within some small posterior loculi (**c**)

the prognosis is worse compared to stage I of the other histologic subtypes [2]. The relationship with endometriosis is strongest (25%) among the ovarian cancers. The tumor may arise within endometriosis (Fig. 10.18), or endometriotic implants may be found commonly in relationship to the tumor or elsewhere in the pelvis [2]. Hypercalcemia as a paraneoplastic syndrome and thromboembolic complications are more common than in other ovarian cancers [41]. Most common gross appearance is a thick-walled unilocular cyst with multiple protruding nodules or a multilocular cystic mass (Fig. 10.19) [2].

Imaging Findings of Epithelial Ovarian Cancers

Epithelial ovarian cancers are typically larger than 4–5 cm at time of presentation. On CT and MRI, they present as a complex cystic or multiloculated ovarian lesion. Although differentiation between the subtypes is not reliably possible by imaging, there might be some differential diagnostic clues. Bilateral ovarian involvement is typically found in serous cystadenocarcinomas, which is the most common ovarian cancer; rarely is it encountered in endometrioid cancer. Psammoma bodies, which can only be detected on CT, are characteristic of serous ovarian cancers. Enhancement of a mural nodule within an endometrioma is highly suggestive of a malignant ovarian neoplasm. Endometriosis is associated with endometrioid, and especially with clear cell cancer. The latter appears most commonly as a large unilocular cyst with one or more solid mural nodules [42]. In endometrioid ovarian cancer, endometrial thickening or abnormal uterine bleeding can also be found.

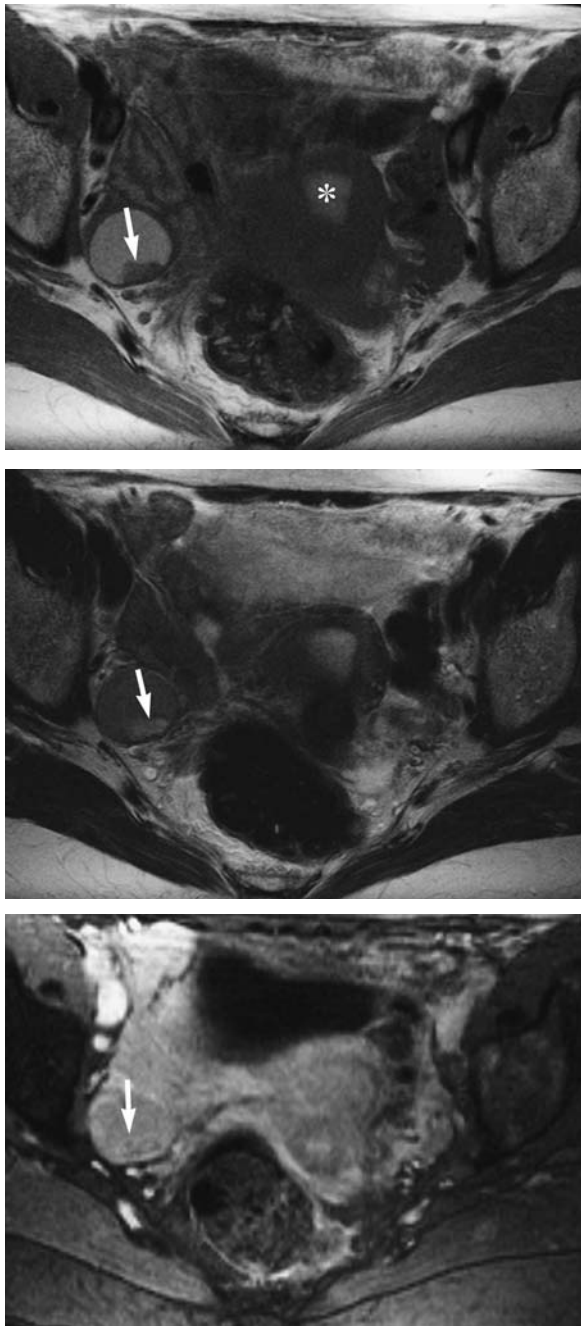

Fig. 10.18a–c. Clear cell carcinoma arising in an endometrioma. Transaxial T1-weighted image (**a**), T2-weighted image (**b**), and contrast-enhanced fat-saturated (FS) T1-weighted image (**c**). A typical endometrioma of the right ovary is demonstrated in **a** and **b**, showing high signal intensity (SI) on T1-weighted image and shading with low SI on the T2-weighted image. Within the posterior wall of the endometrioma a band-like mural lesion (*arrow*) with low SI on T1-weighted image (**a**) and high SI on T2-weighted image (**b**) is seen. Due to contrast enhancement it is obscured in **c**. Contrast enhancement is not found in a clot in endometrioma, but is indicative of a tumor within the endometrial cyst. Hematometra (*asterisk*)

Differential Diagnosis

Benign serous and mucinous cystadenomas are usually entirely cystic and display thin walls and septa. Small papillary projections may also be present in cystadenomas. Metastases, particularly from primary cancer of the appendix or gastrointestinal tract may display similar imaging characteristics as ovarian cancer. Calcifications may also be present in metastases of mucinous adenocarcinoma of the colon and papillary thyroid cancer [39]. Malignant ovarian tumors of other origins may display similar imaging characteristics as ovarian cancer. Age and hormonal effects may help in the differential diagnosis. Other differential diagnoses include benign cystic and/or solid tumors, e.g., cystadenofibroma (Fig. 10.20) and rarely dermoids without fat. Mesothelioma and papillary serous carcinoma of the peritoneum may have an appearance similar to ovarian cancer. Normal size of the ovaries may be a diagnostic clue to exclude ovarian cancer. In case of

Fig. 10.19. Clear cell carcinoma. Parasagittal T2-weighted image shows a large, well-delineated cystic ovarian lesion cephalad of the bladder (*B*), which extends to the midlumbar region. At its anterior wall, broad-based protruding nodules (*arrow*) with a thickness of more than 2 cm are demonstrated, a typical finding of an ovarian malignancy. Courtesy of Dr. M.T. Cunha, Lisbon

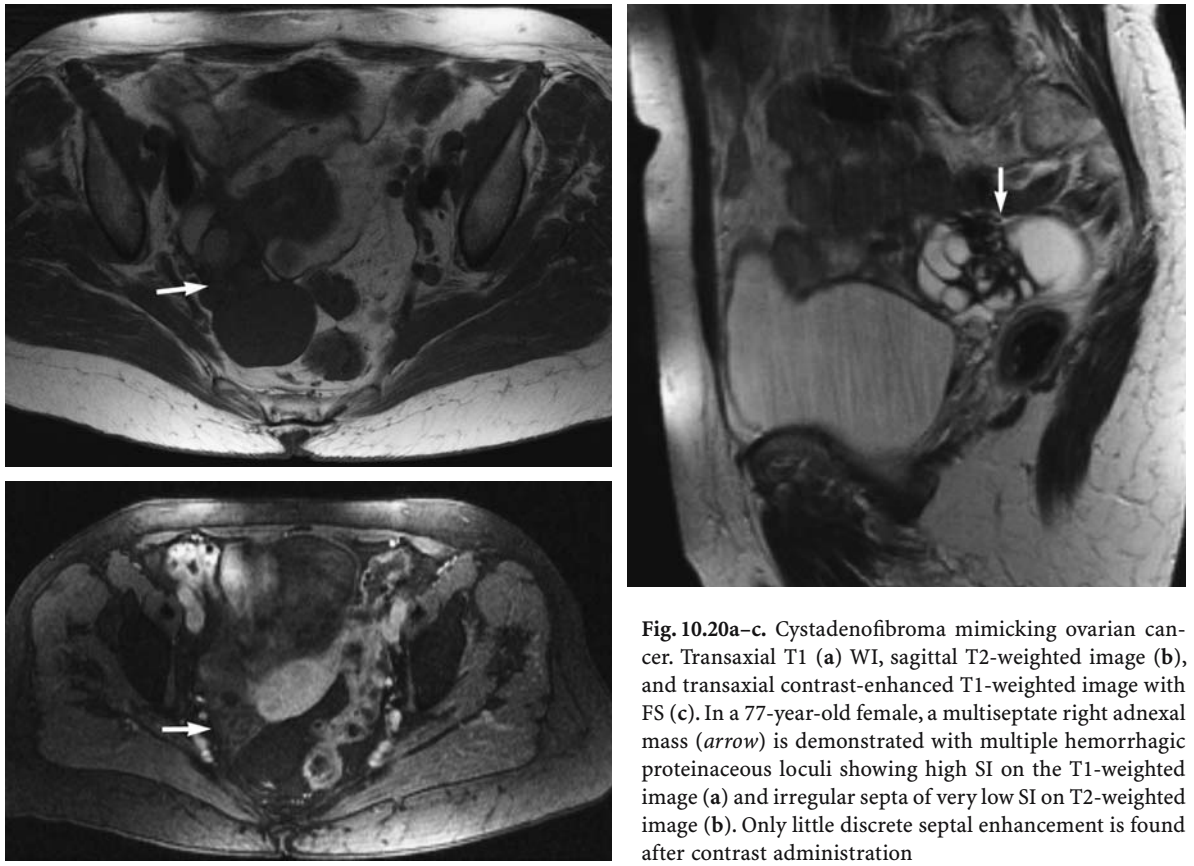

Fig. 10.20a–c. Cystadenofibroma mimicking ovarian cancer. Transaxial T1 (**a**) WI, sagittal T2-weighted image (**b**), and transaxial contrast-enhanced T1-weighted image with FS (**c**). In a 77-year-old female, a multiseptate right adnexal mass (*arrow*) is demonstrated with multiple hemorrhagic proteinaceous loculi showing high SI on the T1-weighted image (**a**) and irregular septa of very low SI on T2-weighted image (**b**). Only little discrete septal enhancement is found after contrast administration

extensive peritoneal disease, differentiation of ovarian cancer from extraovarian pelvic tumors may be difficult, especially by CT. In the majority of cases, tuboovarian abscesses can be distinguished from ovarian cancer based upon imaging and clinical findings. Endometriomas can be differentiated by MRI by typical findings such as shading, thick capsules, and lack of enhancing solid components. However, especially in CT, extensive endometriomas may be a diagnostic problem and mimic ovarian cancer (Fig. 10.21).

10.6.4.1.5 Borderline Tumors

Borderline tumors are epithelial ovarian cancers with low malignant potential. They account for approximately 4%–14% of all ovarian malignancies and present a different entity from invasive epithelial cancers. Serous and mucinous borderline tumors can be distinguished by specific histologic features including epithelial budding, multilayering of the epithelium, increased mitotic activity, nuclear atypia, and lack of stromal invasion cancer [2].

The medium age is 40 years, which is approximately 20 years earlier than for women with epithelial ovarian cancers. Compared to epithelial ovarian cancer, the survival rate stage for stage is much better. A 7-year follow-up of survival of stage I diseases was 99% and for stage II and III disease 92% [4].

Borderline tumors may be large, with diameters ranging from 7 to 20 cm; bilaterality is common. Mucinous tumors of borderline malignant potential tend to be larger, and may be associated with pseudomyxoma peritonei.

Imaging Findings

Borderline tumors tend to be large unilateral or bilateral ovarian tumors that cannot be distinguished from invasive ovarian cancers in CT or MRI. Papillary projections ranging from 10 to 15 mm in size and protrude into the cyst wall are more frequently found in borderline tumors compared to benign and malignant epithelial ovarian tumors (Fig. 10.22) [22]. Rarely, borderline tumors may present as a unilocular cyst larger than 6 cm in size [43].

10.6.4.1.6 Recurrent Ovarian Cancer

Although the initial response to treatment is good, persistence or recurrence of ovarian cancer remains a major problem. This is reflected by the 5-year survival rate for patients with advanced stages of ovarian cancer of 10%–30% [15].

Survival correlates with the disease-free interval before tumor recurrence and the residual disease following primary cytorective surgery [4, 44]. Patients who have a disease-free interval of more than 6 months or 1 year have a markedly improved prognosis. These patients have also been shown to benefit from following secondary cytoreductive surgery [4].

Pelvic recurrences develop after an average of 1.8 years, and hematogenous metastases (liver, spleen, lungs, and brain) after an average of 2.5 years [29]. The pelvis, particularly the vaginal vault and the cul-de-sac, is the most common site of tumor recurrence, and it is followed by abdominal peritoneal implants. Typical abdominal locations include the surface of the diaphragm and liver, paracolic gutters, the large- and small-bowel surface, and mesentery. Because of the surgical technique, omental recurrence is rare. This is also true for pelvic lymph node metastases in recurrent ovarian cancer. Lymph node metastases are typically located in the para-aortal region and found in 18%–33% (Fig. 10.23) [29]. Small- and large-bowel obstruction is a common complication in patients with recurrent ovarian cancer and presents the leading cause of mortality.

Unlike in primary ovarian cancer, recurrent ovarian cancer is not strongly associated with ascites. In one study, ascites was only found in 38% of patients with ovarian cancer, and in the vast majority the amount of fluid detected was small. Furthermore, small amounts of ascites were also demonstrated in patients without evidence of tumor recurrence [45].

Serum tumor markers (CA-125) are pivotal in the follow-up of patients with a history of ovarian cancer. A rising CA-125 level in a patient in a clinically complete remission is highly predictive of recurrence. However, this may precede the median time to physical or radiographic evidence of recurrent disease by 4–6 months [4].

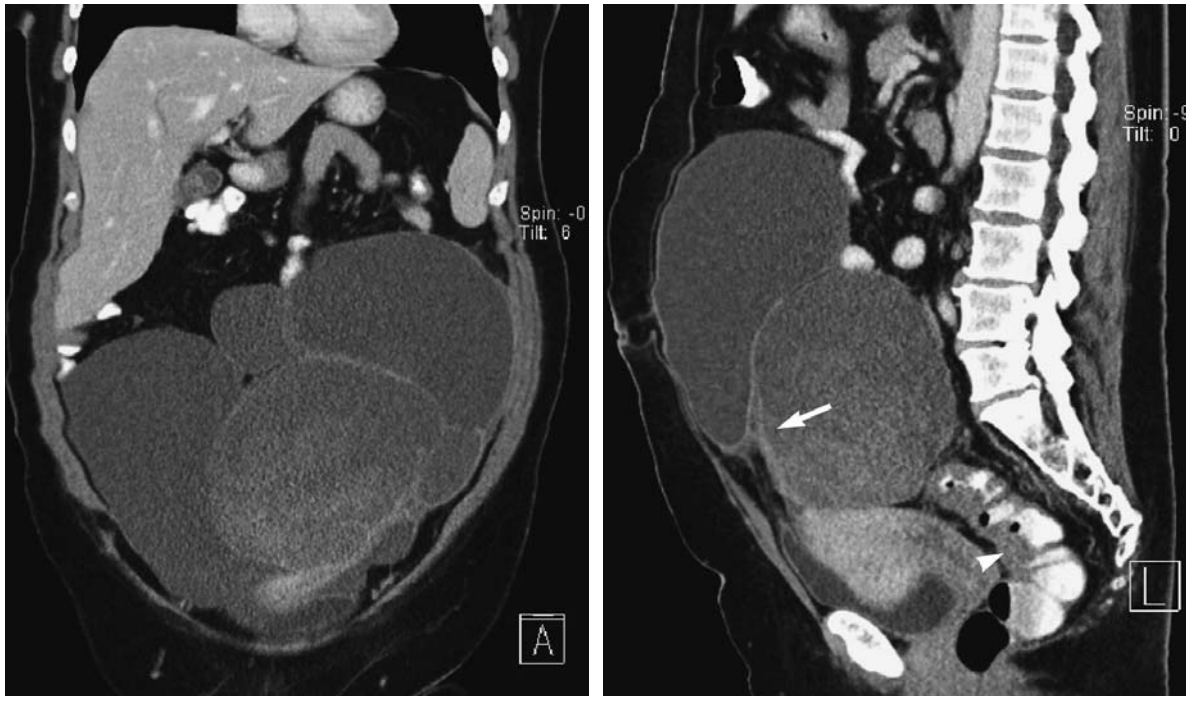

a b

Fig. 10.21a,b. Endometrioma mimicking ovarian cancer in CT. Coronal (**a**) and sagittal CT (**b**). In a 47-year-old woman with elevated tumor markers, a multicystic mass with a diameter of 25 cm occupies the pelvis and midabdomen. Focal mural and septal thickening (*arrow*) and high density within some cysts are demonstrated. There was no evidence of lymph node enlargement or ascites. At surgery, extensive endometriosis of the ovaries and peritoneum was found. Furthermore, mural wall thickening of the rectum and sigmoid colon by endometriosis (*arrowhead*) and thickening of the uterine corpus due to endometriosis was detected (**b**)

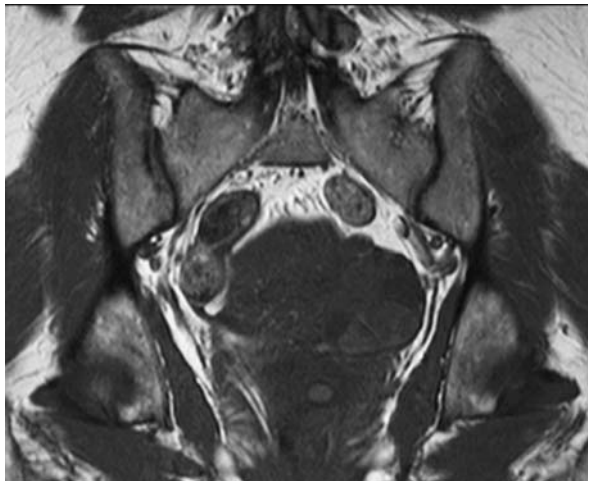

a

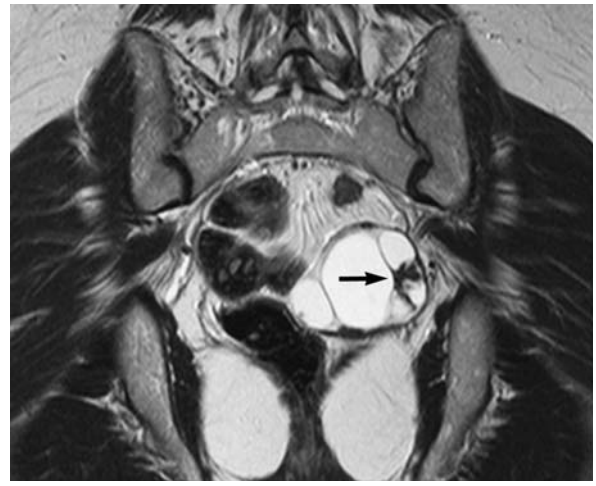

b

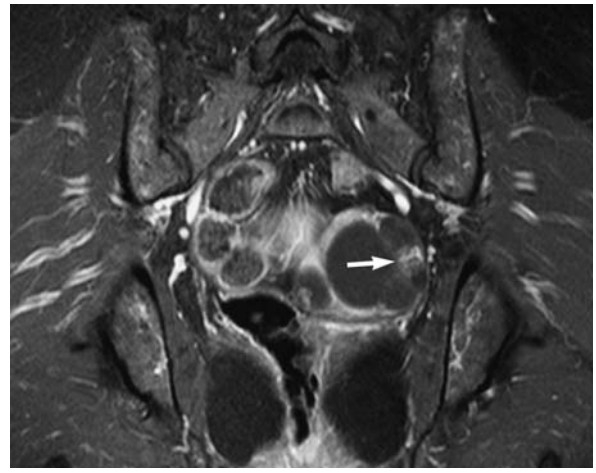

c

Fig. 10.22a–c. Borderline tumor of the left ovary. Coronal T1-weighted image (**a**), T2-weighted image (**b**) and contrast-enhanced T1-weighted image (**c**) with fat saturation. A well-delineated multilocular cystic lesion is seen in the left cul-de-sac displacing the rectum. The loculi contain fluid of high proteinaceous content (**a**) and papillary projections (*arrow*) (**b, c**). The latter are murally located and display low SI on T2-weighted image (**b**) and contrast enhancement (**c**). Papillary projections are more frequently found in borderline tumors than in invasive ovarian cancers. Courtesy of Dr. K. Kinkel, Geneva

a

b

Fig. 10.23a,b. Ovarian cancer recurrence. Coronal CT scans (**a, b**) in a patient with advanced recurrent clear cell cancer show multiple, predominantly cystic peritoneal implants throughout the abdomen and pelvis. The liver surface is compressed by surface implants (*asterisk*) (**a, b**). Multiple enlarged lymph nodes are seen in the right pelvis and root of the mesentery (**b**). Associated findings in this case include bilateral pleural effusion and a thrombus in the left femoral vein

Imaging Findings

Recurrent ovarian cancer most frequently presents as solid, followed by mixed solid and cystic lesions located within the pelvis (Fig. 10.23). Entirely cystic lesions are rarely found [45]. In CT, recurrent disease usually displays moderate contrast enhancement. In MRI, the imaging findings depend on the morphology of the lesions. Usually smaller lesions display low to intermediate SI on T1-weighted images and intermediate to high SI on T2-weighted images (Fig. 10.24). Contrast-enhanced images improve characterization of the architecture of the lesions and facilitate the detection of small peritoneal surface lesions, especially their differentiation from bowel loops. Diffuse or focal peritoneal enhancement presents carcinosis peritonei. The pattern of peritoneal involvement is similar to primary ovarian cancer, with diffuse thin lining of the peritoneal surfaces 2–5 mm thick to plaquelike lesions or nodules emerging from the peritoneal surfaces. Diffuse ascites is found less commonly in localized recurrent ovarian cancer and presents usually a sign of diffuse peritoneal recurrent disease. Omental caking is usually encountered only in patients who had received primary chemotherapy treatment. Small-bowel obstruction is a common complication as ovarian cancer advances and occurs in 5%–42% of ovarian cancer cases [46]. Signs of malignant bowel

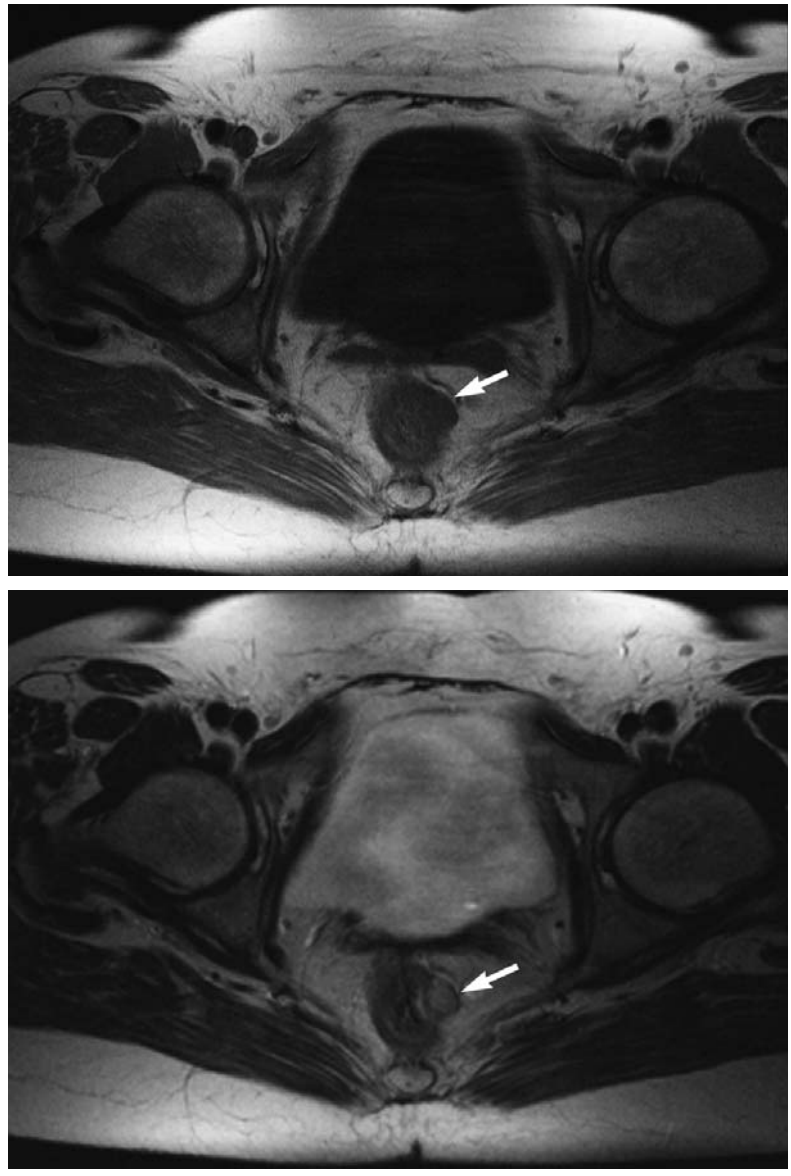

Fig. 10.24a,b. Recurrent ovarian cancer. Transaxial T1-weighted image (**a**) and T2-weighted image (**b**) at the level of the vaginal stump. In a patient with a history of surgery and chemotherapy for ovarian cancer, rising tumor markers were found. The vaginal stump is unremarkable; however, a focal nodular surface lesion of the left rectal wall (*arrow*) is demonstrated, which is protruding minimally into the mesorectal fat. This metastasis was the only manifestation of recurrent ovarian cancer

obstruction include bowel dilatation, an obstructing mass, focal mural thickening, and peritoneal carcinomatosis [46]. A pseudo-small-bowel obstruction pattern can mimic small-bowel obstruction. It is typically encountered late in the course of the disease and is caused by tumor infiltration of the myenteric plexus of the small bowel [4].

Secondary cytoreduction, which is usually performed in pelvic recurrence, is only considered successful when complete resection without a residual tumor is possible. Preoperatively, it is crucial to assess pelvic side wall invasion rather than tumor size [44]. Pelvic sidewall invasion can be excluded when the tumor shows a distance of 3 mm or more to the pelvic sidewall and no involvement of the iliac vessels is found [24].

Differential Diagnosis

Not every solid lesion in a postoperative patient means ovarian cancer recurrence. The combination of CA-125 and a baseline imaging study usually aids in the differential diagnosis. Postoperative hematomas, adhesions between bowel loops, or localized trapped fluid may mimic recurrent disease. Benign forms of diffuse peritoneal thickening such as a result of postoperative inflammatory complications or bacterial peritonitis cannot be differentiated from peritonitis carcinomatosa. Furthermore, chemical peritonitis following intraperitoneal chemotherapy also results in diffuse peritoneal thickening [32].

Value of Imaging

Second look surgery no longer plays a role as a routine procedure in the follow-up of ovarian cancer. Tumor markers, particularly CA-125, play a pivotal role in monitoring patients with ovarian cancer. Imaging in conjunction with this tumor marker is used to assess disease progression and response to therapy. Baseline examinations after surgery or before chemotherapy have been advocated to allow an objective follow-up [47]. However, in many institutions imaging is only performed when tumor markers persist or increase, or when the patients present with clinical symptoms. The exact assessment of the location and volume of recurrent ovarian cancer by imaging has a direct impact on patient management. Only patients with recurrent resectable pelvic disease may be considered as candidates for a secondary cytoreductive surgery. Furthermore, patients can be selected who will benefit from a relieving colostomy [4]. Among the imaging modalities, CT has been widely used for the assessment of recurrent ovarian cancer. MRI may assist in predicting tumor respectability, particularly in the pelvis. Recently, excellent performance has been reported for MRI in predicting the presence of residual ovarian tumors, comparable to the performance of laparotomy and superior to CA-125 values [16]. Abnormal MRI findings with a normal CA-125 value is a strong indicator of residual or recurrent tumor [16]. FDG PET or integrated PET/CT plays an increasing role in the assessment of recurrent ovarian cancer. It is particularly useful in assessing persistent ovarian cancer and serves as a complementary imaging technique when tumor markers are rising and CT or MRI findings are inconclusive or negative [48]. It seems superior to the other imaging techniques in assessing small implants within the mesentery or bowel surface [49].

10.6.4.2 Nonepithelial Ovarian Malignancies

10.6.4.2.1 Malignant Germ Cell Tumors

Malignant germ cell tumors of the ovary are much less common than epithelial ovarian neoplasms. Although germ cell ovarian malignancies account for 2%–3% of all ovarian malignancies, their clinical importance is based upon their potential for cure and the typical age distribution [4]. In women younger than 20 years of age they account for approximately two-thirds of all ovarian malignancies. They are often very large solid tumors with rapid and predominantly unilateral growth [50]. The most frequent sites of dissemination are the peritoneum and retroperitoneal lymph nodes. Compared with epithelial tumors, they have a greater tendency for hematogenous metastases, and liver and lung involvement can be observed at diagnosis. Ascites is only found in approximately 20% of cases [4]. Serum levels of HCG and AFP may assist in the diagnosis and follow-up of some germ cell tumors.

Malignant germ cell tumors comprise, in order of decreasing frequency, dysgerminomas, immature teratomas, endodermal sinus tumors, and embryonal and nongestational choriocarcinomas. The latter three are extremely rare. In these patients, tumor markers may be helpful for assessing response and tumor recurrence. Endodermal sinus tumors secrete AFP. Embryonal carcinomas can secrete both AFP and HCG, whereas pure choriocarcinomas secrete only HCG [4].

10.6.4.2.2 Dysgerminomas

Dysgerminomas present the most common type of malignant germ cell tumors and have been considered the female equivalent of seminoma of the testis. Seventy-five percent occur in early reproductive age, 10% in prepubertal girls, and 15%–20% are diagnosed during pregnancy or postpartally [51]. The vast majority of patients with dysgerminomas are diagnosed with early-stage disease. In contrast to the other germ cell tumor types, dysgerminomas may also occur bilaterally.

Imaging Findings

Dysgerminoma presents as a multilobulated, well-delineated solid lesion. In CT, speckled calcifications may be observed. Furthermore, they may contain low attenuation areas representing necrosis or hemorrhage. Contrast-enhanced CT may also demonstrate strongly enhancing fibrovascular septa. In MRI, the tumor displays low signal intensity on T1-weighted images and intermediate signal with low SI septa and high signal intensity areas of necrosis on T2-weighted images (Fig. 10.25). As in CT, intralesional septa may display strong enhancement [52].

Differential Diagnosis

Differential diagnosis includes solid ovarian tumors in younger age, e.g., granulosa cell tumors and teratomas. In MRI, uterine fibroma and fibrothecoma may display a similar appearance on T2-weighted images; however, contrast enhancement in these tumors is less and delayed. Especially in CT, differentiation of subserosal uterine fibroids from solid dysgerminomas is not possible.

10.6.4.2.3 Immature Teratomas

Immature teratomas or malignant teratomas are the second most common germ cell malignancies. They may rarely be encountered in postmenopausal women. The typical age group is the same as in dermoid cysts, typically young women between 10 and 20 years of age. However, in contrast to benign teratomas, they are extremely rare, with less than 1% consisting of immature teratomas. They are typically large at the time of diagnosis and present as solid or predominantly solid tumors with cystic elements and areas of fat and calcifications. Immature teratomas are associated with dermoid cysts, more commonly in the ipsilateral (26%) than in the contralateral ovary [53]. Immature teratomas contain embryonic tissues and can also occur in combination with other germ cell tumors (mixed germ cell tumors). Yolk sac tumors within immature teratomas give rise to alpha fetoprotein elevation and are an important prognostic factor in these patients [53]. Immature teratomas may also rarely produce steroids and cause pseudoprecosity in prepubertal girls [54].

Imaging Findings

The appearance is variable with heterogenous, predominantly solid lesions or cystic or mixed solid and cystic lesions with scattered or coarse calcifications or hemorrhage [55, 56]. In CT, punctate foci of fat and calcifications are diagnostic clues for the pres-

Fig. 10.25. Dysgerminoma of the right ovary. Sagittal T2-weighted image with FS. In an adolescent, a large, well-delineated solid lesion is located cranially and anterior of the uterus (*U*). It displays predominantly low to intermediate SI on the T2-weighted image. Centrally a region of high signal is seen presenting necrosis; furthermore, multiple septa (*arrows*) of low SI can be identified. The lesions showed intense homogenous contrast enhancement (not shown) and small central necrosis. Small amount of ascites is found between bladder and the tumor. Courtesy of Dr. T.M. Cunha, Lisbon

ence of a teratoma [55]. In case of cystic lesions, they are typically filled with serous fluid and may rarely contain fatty sebaceous material [56]. In MRI, small foci of fat with high SI on T1 (Fig. 10.26) and signal loss on the fat sat sequence are typically found [56]. Capsule penetration allows the differentiation from a mature teratoma [50].

Differential Diagnosis

The presence of fat is the diagnostic clue for the diagnosis of teratomas. Immature teratomas are usually large at presentation. In contrast to the majority of benign teratomas, which are cystic, malignant teratomas tend to be predominantly solid with small foci of fat and scattered calcifications. Elevation of alpha 1 fetoprotein assists in establishing the diagnosis, and is found in 33%–65% of immature teratomas [56]. Concomitant mature and immature teratomas occur in approximately 20% of cases. If no fat is identified immature teratoma cannot be differentiated from ovarian cancer.

10.6.4.2.4 Sex Cord Stromal Tumors

Sex cord stromal tumors derive from coelomic epithelium or mesenchymal cells of the embryonic gonads [54]. Eight percent of all ovarian neoplasms account for this tumor type, with granulosa cell tumors, fibrothecomas, and Sertoli-Leydig cell tumors comprising the majority of these tumors. In contrast

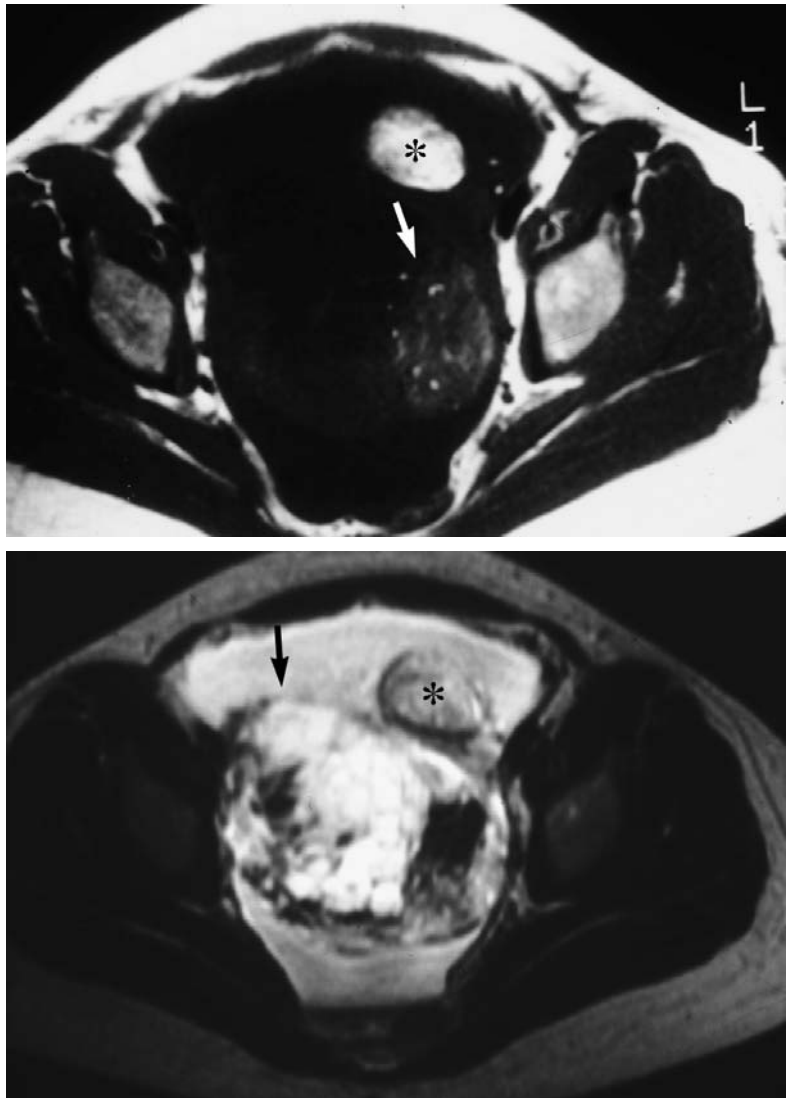

Fig. 10.26a,b. Mature and immature teratoma in a 20-year-old female. T1-weighted image (**a**) and T2-weighted image with FS (**b**) at the acetabular level. Ascites surrounds bilateral ovarian lesions. The left tumor (*asterisk*) represents a benign dermoid with predominantly fatty tissue. Posteriorly an inhomogeneous mixed solid and cystic lesion (*arrow*) with small hemorrhagic loculi is seen, which is better identified on the T2-weighted image (**b**). The tiny spots of high SI on T1-weighted image represent areas of fat (*arrow*, **a**)

to the benign fibrothecomas, granulosa cell tumors are classified as tumors of low-grade malignancy. Sertoli-Leydig cell and steroid tumors may be malignant depending on the degree of differentiation [54]. Sex cord stromal tumors affect all age groups, but are commonly encountered in peri- and postmenopausal women [57]. Their clinical and differential diagnostic importance is based upon their hormone activity. Granulosa cell tumors may typically produce estrogens; Sertoli-Leydig cell tumors and steroid cell tumors are androgen-producing tumors. The majority of sex cord stromal tumors are confined to the ovary at the time of diagnosis [58].

10.6.4.2.5 Granulosa Cell Tumors

Granulosa cell tumors are classified as neoplasm of a low-grade malignancy. Two subgroups of granulosa cell tumors, the juvenile and adult subtype, which differ in several important aspects, can be differentiated. Adult granulosa cell tumors account for 1%–2% of all ovarian tumors and for 95% of all granulosa cell tumors [54]. Granulosa cell tumors are the most common ovarian tumors with estrogen production. Juvenile granulosa cell tumors are hormonally active in 80% and occur typically before the age of 30. The vast majority are found in prepubertal girls who present with the signs of precocious pseudopuberty with development of breasts and pubic and axillary hair. An association with Ollier's disease (enchondromatosis) and Maffucci's syndrome (enchondromatosis and hemangiomatosis) has been reported in some cases [54].

The adult granulosa cell tumors usually occur after the age of 30 years and have their peak incidence in the perimenopausal age [54]. Because of their estrogen activity, they can become clinically apparent with abnormal uterine bleeding and endometrial hyperplasia. Endometrial cancer is associated with these tumors in 5%–25% of cases [58]. Both types of granulosa cell tumors are typical unilateral ovarian tumors that vary considerably in size and show an average diameter of approximately 12 cm [54].

In adult granulosa cell tumors, late recurrence years after the initial therapy tumor manifestation may be seen. The recurrent tumor is typically confined to the pelvis and abdomen (Fig. 10.27). However, distant metastases to the bone, supraclavicular lymph nodes, liver, and lungs have been reported [29].

Imaging Findings

Granulosa cell tumors can display a broad spectrum from entirely cystic to completely solid ovarian lesions (Fig. 10.28) [22]. The latter may display homogenous contrast enhancement and high SI on T2-weighted images. They may also manifest as a solid and cystic neoplasm, and cysts may contain hemorrhagic fluid. The adult type of granulosa cell tumor manifests mostly as a predominantly sponge-like cystic multilocular tumor with blood clots and solid tissue [59].

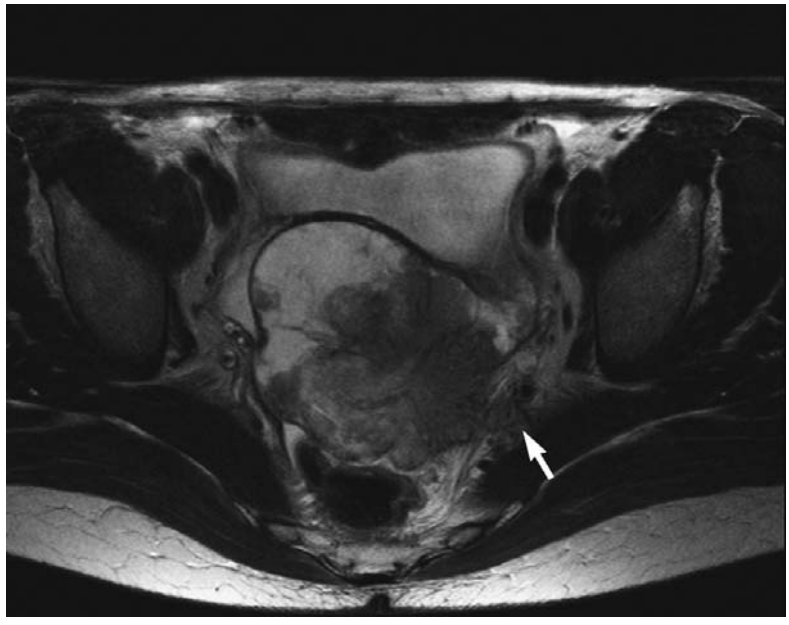

Fig. 10.27. Late recurrence of granulosa cell tumor. Transaxial T2-weighted image in a 45-year-old patient with a history of hysterectomy and resection of a granulosa cell tumor 16 years before. Recurrent granulosa cell tumor is identified as a solid and cystic lesion above the vaginal vault. The right border is well defined, the left posterior margin shows irregular contours (*arrow*) extending to the posterior pelvic sidewall. Small amounts of ascites are demonstrated in the pelvis. At surgery, invasion of the iliac internal vessels was confirmed

Fig. 10.28. Juvenile type of granulosa cell tumor. CT in a 17-year-old girl who presented with primary amenorrhea. A large, well-defined cystic ovarian tumor with multiple irregular septations and solid areas is demonstrated in the midpelvis. Small amounts of ascites (*asterisk*) without evidence of peritoneal seeding at surgery

10.6.4.2.6 Sertoli-Leydig Cell Tumor

Sertoli-Leydig cell tumors account for less than 0.5% of ovarian tumors. The majority (75%) of Sertoli-Leydig cell tumors occur in women younger than 30 years [57]. Less than 10% are found in women over 50 years of age [54]. Although virilization caused by androgen production is the most striking clinical feature, it occurs in only one-third of patients [54]. Other symptoms include menstrual irregularities or abnormal bleeding. Approximately 50% of women with Sertoli-Leydig tumors have no endocrine effects. Most Sertoli-Leydig cell tumors are unilateral and the majority are diagnosed as stage I disease. They vary in size between 5 and 15 cm (average, 13.5 cm). Some of these tumors, however, may be very small and difficult to detect by imaging, although they cause hormonal effects [60]. Depending upon the degree of differentiation, 1%–59% of Sertoli-Leydig cell tumors were malignant in one series [54]. In contrast to granulosa cell tumors, Leydig cell tumors tend to recur typically within the 1st year after surgery.

Imaging Findings

Sertoli-Leydig cell tumors vary greatly in gross appearance. They tend to be solid, sometimes lobulated masses. They may also appear as predominantly solid masses often with peripheral cysts or as a cystic lesion with polypoid mural structures [57]. Cysts may display a slightly high signal intensity on T1-weighted images. The solid components display intermediate to high SI on T2-weighted images and good contrast enhancement in MRI and CT [22]. Rarely, these tumors may manifest as a cystic lesion [60]. Less differentiated types of Sertoli-Leydig cell tumors tend to display an inhomogenous architecture with areas of necrosis and hemorrhage.

10.6.4.2.7 Ovarian Lymphoma

Although the ovaries are not infrequently found to be involved by malignant lymphoma at autopsy, enlargement of the ovaries is rare. Less than 1% of patients with lymphoma initially present with unilateral or bilateral ovarian tumors [61]. Ovarian lymphoma is almost always a manifestation of a systemic disease, most commonly of B-cell lymphomas. Primary lymphoma of the ovary without lymph node or bone marrow involvement is extremely rare. It is encountered most commonly in premenopausal women.

Imaging Findings

Lymphomas appear as unilateral or more commonly as bilateral ovarian solid, often homogenous masses without ascites [62]. In CT, they appear as well defined solid masses with mild contrast enhancement. In MRI, they display intermediate signal on T1 and low to intermediate SI on T2-weighted images. Similar to CT, mild contrast enhancement is noted (Fig. 10.29).

Differential Diagnosis

Ovarian cancer may resemble ovarian lymphoma. Bilateral involvement is most commonly found in

serous, undifferentiated ovarian cancers, and in borderline tumors. Ovarian cancer displays a heterogenous architecture, typically with solid and cystic elements. Furthermore, signal intensity on the T2-weighted image is often very high, and ascites is found in the majority of cases. Metastases may also present as a unilateral or bilateral solid ovarian masses. They usually display strong contrast enhancement and central necrosis or cysts. Clinical history, evidence of multiple lymph nodes, and splenomegaly support the diagnosis of lymphoma.

10.6.4.3 Ovarian Metastases

Approximately 5%–15% of malignant ovarian tumors are metastases to the ovaries. Colon, stomach, breast, and lymphoma are the most commonly encountered neoplasm to metastasize to the ovaries. Metastases from numerous other sites including melanoma, endometrial cancer, cancer of the pancreas, gallbladder, and carcinoid account for less common sources for ovarian metastases [63]. Ovarian metastases seem more common in premenopausal women because of higher vascularity of the ovaries in this age group, and they may be associated with hormonal activity [63]. Although metastases may occur unilaterally (especially in endometrial cancer), bilateral involvement is more typical and occurs in up to 75% of cases [14]. Approximately 50% of ovarian metastases consist of Krukenberg tumors, which display characteristic features at histopathology and imaging. Krukenberg tumors originate from the stomach, gastrointestinal tumors, or the breast, and contain mucin-secreting signet ring cells surrounded by ovarian stroma. Compared to other neoplasms, Krukenberg tumors have a fourfold risk to metastasize into the ovaries. In patients with a history of Krukenberg tumors, complex ovarian tumors should be highly suspicious of metastases. In a multicenter study assessing 86 patients with primary ovarian and 24 patients with secondary cancers, only multilocularity favored the diagnosis of a primary ovarian cancer [64].

Ovarian metastases are often asymptomatic. They may rarely even precede the primary neoplasm. In general, ovarian metastases are associated with a poor prognosis and the majority of patients will die within the first year after detection [54].

10.6.4.3.1 Imaging Findings

On imaging, two types of ovarian metastases may be differentiated [14]. Krukenberg tumors display characteristic imaging features that typically include bilateral oval or kidney-shaped tumors, which tend to preserve the contour of the ovary. They are solid or predominantly solid with central necrosis or cysts and may attain a large size. On MRI, they display medium signal intensity on T1-weighted images, and an inhomogeneous low to intermediate SI on T2-weighted images (Fig. 10.30) [65, 66]. In CT and

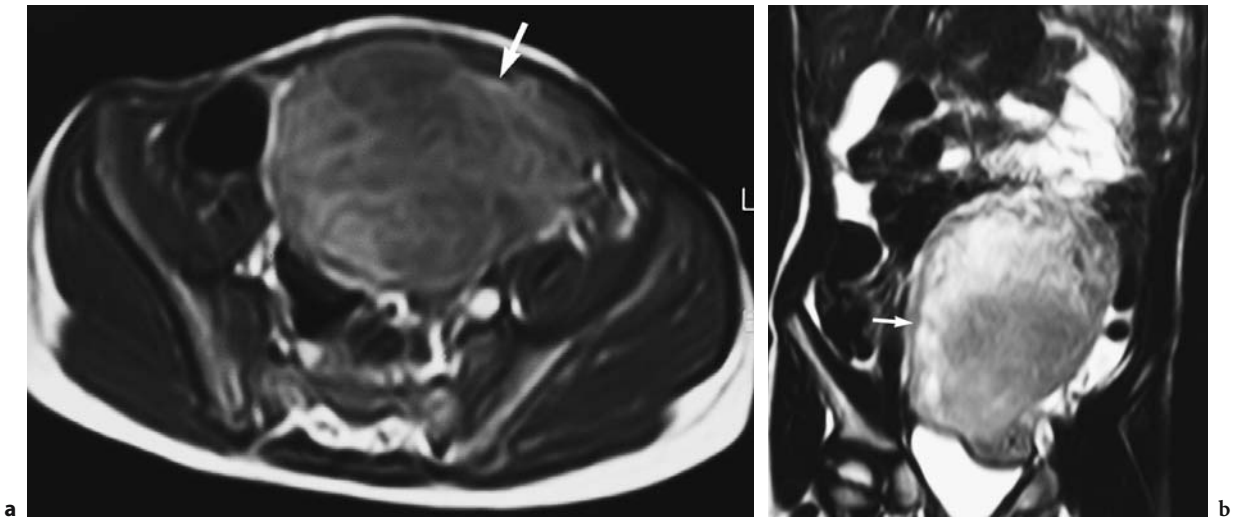

Fig. 10.29a,b. Ovarian lymphoma in a child. Contrast-enhanced T1-weighted image in the midpelvis (**a**) and coronal T2-weighted image (**b**) Non-Hodgkin lymphoma only confined to the left ovary presents as a large solid mass (*arrow*) with moderate contrast enhancement (**a**) and inhomogenous low to intermediate SI on T2-weighted image (**b**)

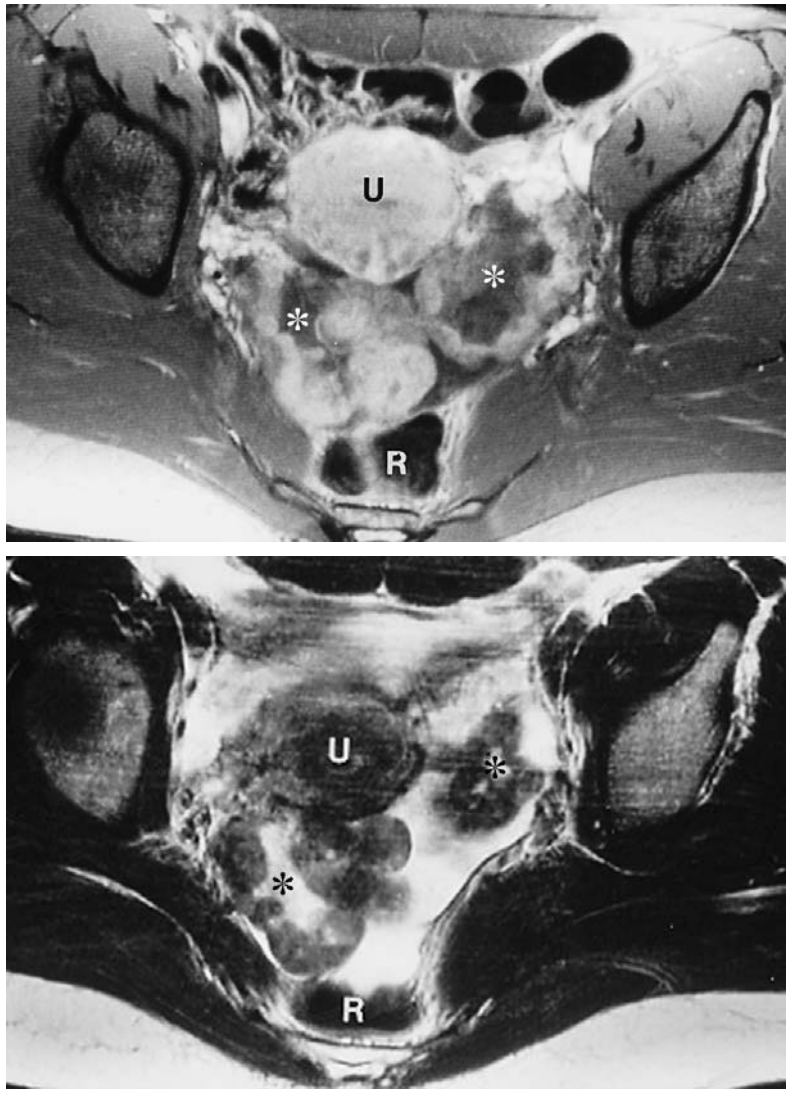

Fig. 10.30a,b. Bilateral Krukenberg tumors. Contrast-enhanced T1-weighted image (**a**) and T2-weighted image (**b**) show bilateral ovarian lesions with the typical imaging features of Krukenberg tumors. These include lobulated solid lesions with central necrosis (*asterisks*), which display strong contrast enhancement (**a**) and low SI of the solid components on T2-weighted image (**b**).The lesions are well delineated due to ascites. *R*, rectum. *U*, uterus. Courtesy of Dr. A. Heuck, Munich

contrast-enhanced MRI, they tend to show strong enhancement of solid components or septations.

Metastatic cancers different from Krukenberg tumors may have a variable appearance resembling other malignant ovarian lesions with cystic and mixed cystic and solid patterns [64, 67].

Colon cancer metastases commonly present as unilateral or bilateral, multiloculated, predominantly cystic tumors (Fig. 10.31) [63]. Presence of nodules or multinodularity at the ovarian surface may also be a sign of metastatic ovarian involvement. Ascites may be present.

The presence of another tumor outside the ovaries should warrant the diagnosis of metastases to the ovaries if the pattern of spread is atypical for ovarian cancer. In particular, the presence of pulmonary and hepatic metastases in absence of extensive peritoneal spread is unusual for ovarian cancer and favors another primary neoplasm [54].

10.6.4.3.2 Differential Diagnosis

Confident distinction between primary and metastatic ovarian cancers is not possible because of overlapping findings in imaging. Bilateral, sharply delineated, purely solid or predominantly solid tumors with necrosis strongly favor the diagnosis of a metastatic ovarian tumor, most likely Krukenberg tumors [68]. Contrast uptake aids in the differentiation of solid ovarian metastases from stromal tumors. Stromal tumors typically display a mild and delayed contrast uptake [69]. If metastases are cystic

Fig. 10.31. Metastases from colon cancer. Sagittal CT shows a well-delineated mixed cystic and solid ovarian mass (*arrow*), which abuts the uterus fundus and elevates small bowel loops. No ascites was found in the pelvis or abdomen. In this patient with stage T4 colon cancer, differentiation of metastasis from ovarian cancer is not possible by imaging

and hemorrhagic, they may resemble endometriomas, which also occur in younger women. However, distinct contrast enhancement is not found in endometriomas. Abscesses usually present with different clinical features than the clinically silent metastases.

10.6.4.4 Fallopian Tube Cancer

Primary malignant neoplasms of the fallopian tube are extremely rare and account for only 0.3%–1.1% of all gynecologic cancers [4]. Most fallopian tube carcinomas present as papillary serous adenocarcinomas. The intraperitoneal spread of fallopian tube carcinomas is similar to that of epithelial ovarian cancer. However, there seems to be a higher propensity for distant metastases [4]. In contrast to ovarian cancer, the majority of patients with tubal carcinoma are diagnosed at an early stage. Because of pain caused by tubal distension or abnormal uterine bleeding, tubal cancer often becomes clinically apparent early. Most fallopian tube cancers arise from the ampullary part of the fallopian tube and may cause tubal occlusion. In approximately 50% of all cases, fallopian tube cancer resembles hydrosalpinx and is often mistaken as such at surgery [70].

10.6.4.4.1 Imaging Findings

A unilateral adnexal complex cystic or solid mass associated with hydrosalpinx is the most common finding. CT and MR demonstrate complex solid and cystic enhancing masses similar to ovarian cancer. A cystic tubular structure with interdigitating septa adjacent to the mass represents the dilated tube. Signal intensity on T1 and T2 higher than serous fluid suggests hematosalpinx. Occasionally, focal nodularity within a hydrosalpinx may be found in fallopian cancer. Common associated findings are distension of the uterine cavity and ascites [70]. Peritoneal metastases are similar to those in ovarian cancer. Lymph node metastases may be found more often than in ovarian cancer.

10.6.4.4.2 Differential Diagnosis

Primary ovarian cancers cannot be reliably differentiated from fallopian tube cancers; however, the latter are exceedingly rare. In presence of associated hydrosalpinx, tubal cancer may mimic ovarian cancer with cystic and solid components. Especially with T2-weighted images, however, identification of the cystic areas representing the loops of the distended tube is usually possible. Metastases to the fallopian tubes, which result most commonly from direct extension of gynecologic cancers, cannot be reliably differentiated from primary fallopian tube cancers. Rarely, leiomyomas of the fallopian tube may be encountered, which resemble ovarian stromal tumors or fibroids of the broad ligament.

References

1. American Cancer society (2004) Ovarian cancer facts and figures: 2004. American Cancer Society, Atlanta
2. Seidman JD, Russell P, Kurman RJ (2002) Surface epithelial tumors of the ovary. In: Kurman RJ (ed) Blaustein's pathology of the female genital tract. Springer Verlag, Berlin Heidelberg New York pp 791–904
3. Hensley ML, Alektiar KM, Chi DS (2001) Ovarian and fallopian-tube cancer. In: Barakat RR, Bevers MW, Gershenson, HoskinsWJ (eds) Handbook of gynecologic oncology. Martin Dunitz, London, pp 243–263
4. Ozols RF, Schwartz PE, Eifel PJ (2001) Ovarian cancer, fallopian tube carcinoma, and peritoneal carcinoma. In: De Vita VT Jr, Hellman S, Rosenberg SA (eds) Cancer: principles and practice of oncology, 6th edn. Lippincott Williams & Wilkins, Philadelphia, pp 1597–1632
5. Boyd J (1998) Molecular genetics of hereditary ovarian cancer. Oncology 12:399–406
6. Chung DC, Rustgi AK (2003). The hereditary nonpolyposis colorectal cancer syndrome: genetics and clinical implications. Ann Intern Med 138:660–570
7. Bohm-Velez M, Mendelson E, Bree R et al (2000) Ovarian cancer screening. American College of Radiology. ACR Appropriateness criteria. Radiology 215:861–871
8. Scully RE (2000) Influence of origin of ovarian cancer on efficacy of screening. Lancet 355:1028–1029
9. Schwartz PE, Taylor KJ, (1995) Is early detection of ovarian cancer possible? Ann Med 27:519–528
10. Outwater EK, Dunton CJ (1995) Imaging of the ovaries and adnexa: clinical issues and applications of MR imaging. Radiology 194:1–18
11. NIH consensus conference (1995) ovarian cancer: screening, treatment and follow-up. NIH Consensus Development Panel on Ovarian Cancer. JAMA 273:491–497
12. Koonings PP, Campbell K, Mishell DR, Grimes DA (1989) Relative frequency of primary ovarian neoplasm: a 10-year review. Obstet Gynecol 74:921–926
13. Bairey O, Blickstein D, Stark P et al (2003) Serum CA 125 as a prognostic factor in non-Hodgkin's lymphoma. Leuk Lymphoma 44:1733–1738
14. Togashi K (2003) Ovarian cancer: the role of US, CT and MRI. Eur Radiol 13 [Suppl 4]:L87–L104
15. Cannistra SA (2004) Cancer of the ovary. N Engl J Med 351:2519–2529
16. Low RN, Duggan B, Barone RM et al (2005) Treated ovarian cancer: MR imaging, laparotomy assessment, and serum CA-125 values compared with clinical outcome at 1 year. Radiology 235:918–927
17. Buy JN, Ghossain MA, Sciot C et al (1991) Epithelial tumors of the ovary: CT findings and correlation with US. Radiology 178:811–818
18. Sohaib SAA, Sahdev A, Van Trappen et al (2003) Characterization of adnexal lesions on MRI. AJR Am J Roentgenol 180:1297–1304
19. Stevens SK, Hricak H, Stern JL (1991) Ovarian lesions: detection and characterization with gadolinium-enhanced MRI at 1.5 T. Radiology 181:481–488
20. Komatsu KI, Konishi I, Mandai M et al (1996) Adnexal masses: transvaginal US and gadolinium-enhanced MR imaging assessment of intratumoral structure. Radiology 198:109–115
21. Hricak H, Chen M, Coakley FV et al (2000) Complex adnexal masses: detection and characterization with MRI: multivariate analysis. Radiology 214:39–46
22. Jung SE, Lee JM, Rha SE et al (2002) CT and MR imaging of ovarian tumors with emphasis on differential diagnosis. Radiographics 22:1305–1325
23. Coakley FV, Choi PH, Gougoutas CA et al (2002) Peritoneal metastases: detection with spiral CT in patients with ovarian cancer. Radiology 223:495–499
24. Forstner R, Hricak H, Occhipinti K et al (1995) Ovarian cancer: staging with CT and MRI. Radiology 197:619–626
25. Woodward PJ, Hosseinzadeh K, Saenger JS (2004) Radiologic staging of ovarian carcinoma with pathologic correlation. Radiographics 24:225–246
26. Shen-Gunther J, Mannel RS (2002) Ascites as a predictor of ovarian malignancy .Gynecol Oncol 87:77–83
27. Outwater EK, Wilson KM, Siegelman ES, Mitchell DG (1996) MRI of benign and malignant gynecologic disease: significance of fluid and peritoneal enhancement in the pelvis at MR imaging. Radiology 200:483–488
28. Walkey MM, Friedman AC, Sohotra P et al (1988) CT manifestations of peritoneal carcinosis. AJR Am J Roentgenol 150:1035–1041
29. Burghardt E (1993) Epithelial ovarian cancer. Recurrence. In: Burghardt E (ed) Surgical gynecological oncology. Thieme, Stuttgart, p 494
30. Tempany CM, Zou KH, Silverman et al (2000) Staging of advanced ovarian cancer: comparison of imaging modalities-report from the Radiology Oncology Group. Radiology 215:761–767
31. Meyer JI, Kennedy AW, Friedman R et al (1995) Ovarian carcinoma: value of CT in predicting success of debulking surgery. AJR Am J Roentgenol 165:875–878
32. Low RN, Sigeti JS (1994) MR imaging of peritoneal disease: comparison of contrast-enhanced fast multiplanar spoiled gradient-recalled and spin echo sequences. AJR Am J Roentgenol 163:1131–1140
33. Low RN, Saleh F, Song SYT et al (1999) Treated ovarian cancer: comparison of MR imaging with serum CA-125 level and physical examination: a longitudinal study. Radiology 211:519–528
34. Low RN, Semelka RC, Worawattanakul S et al (1999) Extrahepatic abdominal imaging in patients with malignancy: comparison of MRI and helical CT with subsequential surgical correlation. Radiology 210:625–632
35. Bristow RE, Tomacruz RS, Armstrong DK et al (2002) Survival effects of maximal cytoreductive surgery for advanced ovarian carcinoma during the platinum era: a meta-analysis. J Clin Oncol 20:1248–1259
36. Huober J, Meyer A, Wagner U, Wallwiener D (2002) The role of neoadjuvant chemotherapy and interval laparotomy in advanced ovarian cancer. Cancer Res Clin Oncol 128:153–160
37. Quayyum A, Coakley FV, Westphalen AC et al (2005) Role of CT and MR imaging in predicting optimal cytoreduction of newly diagnosed primary epithelial ovarian cancer. Gynecol Oncol 96:301–305
38. Mitchell DG, Hill MC, Hill S et al (1986) Serous carcinoma of the ovary: CT identification of metastatic calcified implants. Radiology 158:649–652
39. Kawamoto S, Urban BA, Fishman EK (1999) CT of epithelial ovarian tumors. Radiographics 19:S85–S102

40. Tanaka YO, Yoshizako T, Nishida M et al (2000) Ovarian carcinoma in patients with endometriosis: MR imaging findings. AJR Am J Roentgenol 175:1423–1430
41. Hricak H, Reinhold C, Ascher SM (2004) Ovarian clear cell carcinoma. In: Hricak H, Reinhold C, Ascher SM (eds) Gynecology top 100 diagnoses. WB Saunders Company, Amirsys, Salt Lake City, pp 104–106
42. Matsuoka Y, Ohtomo K, Araki T et al (2001) MR imaging of clear cell carcinoma of the ovary. Eur Radiol 11:946–951
43. Exacoustos C, Romanini ME, Rinaldo D et al (2005) Preoperative sonographic features of borderline ovarian tumors. Ultrasound Obstet Gynecol 25:50–59
44. Funt AS, Hricak H (2003) Ovarian malignancies. TMRI 14:329–338
45. Forstner R, Hricak H, Azizi L et al (1995) Ovarian cancer recurrence: value of MR imaging. Radiology 196:715–720
46. Low RN, Chen SC, Barone R (2003) Distinguishing benign from malignant bowel obstruction in patients with malignancy: findings at MRI. Radiology 228:157–165
47. Johnson RJ (1993) Radiology in the management of ovarian cancer. Clin Radiol 48:75–82
48. Sironi S, Messa C, Mangili G et al (2004) Integrated FDG PET/CT in patients with persistent ovarian cancer: correlation with histologic findings. Radiology 233:433–440
49. Kubich-Huch RA, Dorffler W, von Schulthess GK et al (2000) Value of FDG positron emission tomography, computed tomography, and magnetic resonance imaging in diagnosing primary and recurrent ovarian cancer. Eur Radiol 10:761–767
50. Brammer HM, Buck JL, Hayes WS et al (1990) Malignant germ cell tumors of the ovary: radiologic pathologic correlation. Radiographics: 10715–10724
51. Hricak H, Reinhold C, Ascher SM (2004) Ovarian dysgerminomas. In: Hricak H, Reinhold C, Ascher SM (eds) Gynecology top 100 diagnoses. WB Saunders Company, Amirsys, Salt Lake City, pp 98–100
52. Tanaka YU, Kurosaki Y, Nishida M et al (1994) Ovarian dysgerminoma: MR and CT appearance. J Comput Assist Tomogr 18:443–448
53. Heifetz SA, Cushing B, Giller R et al (1998) Immature teratomas in children: pathologic considerations. Am J Surg Pathol 22:1115–1124
54. Young RH, Scully RE (2002) Sex-cord-stromal, steroid cell, and other ovarian tumors. In: Kurman RJ (ed) Blaustein's pathology of the female genital tract, 5th edn. Springer, Berlin Heidelberg New York, pp 905–965
55. Bazot M, Cortez A, Sananes S, Boudghene F et al (1999) Imaging of dermoid cysts with foci of immature tissue. J Comput Assist Tomogr 23:703–706
56. Yamaoka T, Togashi K, Koyama T et al (2003) Immature teratoma of the ovary: correlation of MR imaging and pathologic findings. Eur Radiol 13:313–319
57. Tanaka YO, Tsunoda H, Kitagawa et al (2004) Functioning ovarian tumors: direct and indirect findings at MRI. Radiographics 24:S147–S166
58. Outwater EK, Wagner BJ, Mannion C et al (1998) Sex cord-stromal and steroid cell tumors of the ovary. Radiographics 18:1523–1546
59. Kim SH (2002) Granulosa cell tumor of the ovary: common findings and unusual appearances on CT and MR. J Comput Assist Tomogr 26:756–761
60. Outwater EK, Marchetto B, Wagner BJ (2000) Virilizing tumors of the ovary: imaging features. Ultrasound Obstet Gynecol 15:365–371
61. Monterroso V, Jaffe ES, Merino MJ et al (1993) Malignant lymphoma involving the ovary. A clinico-pathologic analysis of 39 cases. Am J Surg Pathol 17:154–170
62. Ferrozzi F, Tognini G, Bova D et al (2000) Non-Hodgkin lymphomas of the ovaries: MR findings. J Comput Assist Tomogr 24:416–420
63. Young RH, Scully RE (2002) Metastatic tumors of the ovary. In: Kurmann RJ (ed) Blausteins's pathology of the female genital tract, 5th edn. Springer, Berlin Heidelberg New York, pp 1063–1101
64. Brown DL, Zou KH, Tempany CMC et al (2001) Primary versus secondary ovarian malignancy: imaging findings of adnexal masses in the radiology diagnostic oncology group study. 219:213–218
65. Ha HK, Baek SY, Kim SH et al (1995) Krukenberg's tumors of the ovary: MR imaging features. AJR Am J Roentgenol 164:1435–1439
66. Kim SH, Kim WH, Park KL et al (1996) CT and MR findings of Krukenberg tumors: comparison with primary ovarian tumors. J Comput Assist Tomogr 20:393–398
67. Megibow AJ, Hulnik DH, Bosniak MA et al (1985) Ovarian metastases: computed tomographic appearances. Radiology 156:161–164
68. Alcazar JL, Galan MJ, Ceamanos C et al (2003). Transvaginal gray scale and color Doppler sonography in primary ovarian cancer and metastatic tumors to the ovary. J Ultrasound Med 22:243–247
69. Troiano RN, Lazzarini KM, Scoutt LM et al (1997) Fibroma and fibrothecoma of the ovary: MR imaging findings. Radiology 204:795–798
70. Kawakami S, Togashi K, Kimura I et al (1993) Primary malignant tumor of the fallopian tube: appearance at CT and MR imaging. Radiology 186:503–508